INFECTIOUS DISEASE

Preferential induction of cross-group influenza A hemagglutinin stem–specific memory B cells after H7N9 immunization in humans

Sarah F. Andrews,[1]* M. Gordon Joyce,[1] Michael J. Chambers,[1] Rebecca A. Gillespie,[1] Masaru Kanekiyo,[1] Kwanyee Leung,[1] Eun Sung Yang,[1] Yaroslav Tsybovsky,[2] Adam K. Wheatley,[3] Michelle C. Crank,[1] Jeffrey C. Boyington,[1] Madhu S. Prabhakaran,[1] Sandeep R. Narpala,[1] Xuejun Chen,[1] Robert T. Bailer,[1] Grace Chen,[1] Emily Coates,[1] Peter D. Kwong,[1] Richard A. Koup,[1] John R. Mascola,[1] Barney S. Graham,[1] Julie E. Ledgerwood,[1] Adrian B. McDermott[1]*

Antigenic drift and shift of influenza strains underscore the need for broadly protective influenza vaccines. One strategy is to design immunogens that elicit B cell responses against conserved epitopes on the hemagglutinin (HA) stem. To better understand the elicitation of HA stem–targeted B cells to group 1 and group 2 influenza subtypes, we compared the memory B cell response to group 2 H7N9 and group 1 H5N1 vaccines in humans. Upon H7N9 vaccination, almost half of the HA stem–specific response recognized the group 1 and group 2 subtypes, whereas the response to H5N1 was largely group 1–specific. Immunoglobulin repertoire analysis of HA-specific B cells indicated that the H7N9 and H5N1 vaccines induced genetically similar cross-group HA stem–binding B cells, albeit at a much higher frequency upon H7N9 vaccination. These data suggest that a group 2–based stem immunogen could prove more effective than a group 1 immunogen at eliciting broad cross-group protection in humans.

INTRODUCTION

Serious influenza disease is caused by two genera of viruses in the family Orthomyxoviridae designated as influenza virus A and B. Type A strains, which are responsible for influenza pandemics, are further subdivided on the basis of the viral glycoprotein hemagglutinin (HA) sequence into group 1 and group 2 subtypes, and each subtype has many strains. Antigenic drift and shift of the viral surface proteins HA and neuraminidase produce new antigenically distinct strains that thwart life-long immunity and present a constant threat of pandemics. Although HA serves as the major target for protective antibodies, HA is genetically and antigenically variable between strains, even within a subtype, and heterosubtypic immunity has been difficult to achieve. There is even greater antigenic distance between subtypes in group 1 and group 2. Exposure to seasonal influenza strains, either by infection or vaccination, elicits dominant B cell responses that target the hypervariable head domain, resulting in strain-specific antibody responses. However, subdominant B cell responses targeting the HA stem region are also generated. These HA stem–specific responses have been intensely investigated in recent years, and isolated monoclonal antibodies (mAbs) have demonstrated broad neutralization across multiple influenza subtypes, including across groups (*1*–*5*). Several vaccine strategies are being explored that target elicitation of B cell responses directed toward the stem region of the HA molecule (*6*–*11*).

The B cell responses targeting the HA stem are dominated by the HA head–specific response after seasonal infection or vaccination. However, upon exposure to novel influenza strains for which humans have little to no preexisting HA head–specific immunity, HA stem–specific responses are more prevalent. For example, after exposure to the novel 2009 pandemic H1N1 or avian influenza virus H5N1, HA stem–specific B cells generated to conserved regions shared by seasonal strains are preferentially expanded (*12*–*16*). Characterization of the HA stem–specific B cell immunoglobulin (Ig) repertoire has shown that human antibodies able to bind the H1N1 and H5N1 HA stem predominantly derive from the VH1-69 heavy chain (*5*, *12*, *17*). Isolation and cocrystallization of HA and VH1-69 antibodies revealed the molecular constraints of binding to the HA stem of group 1 subtypes. Specifically, critical hydrophobic residues in the VH1-69 germline–encoded CDRH2 aided by elements in the CDRH3 are sufficient for initial binding of this variable heavy (VH) gene to the group 1 stem, making it a robust and dominant response to the HA stem of group 1 subtypes (*15*, *18*–*20*). A glycan at $Asn38_{HA2}$ conserved in the HA stem of most group 2 subtypes is thought to prevent most group 1 heterosubtypic antibodies from binding subtypes in group 2 (*3*, *21*).

Previously, only a handful of human HA stem–reactive antibodies capable of binding strains from multiple subtypes in either group 2 or both group 1 and group 2 had been described with diverse molecular characteristics and modes of HA stem recognition (*1*, *2*, *14*, *21*–*23*). However, we recently characterized the repertoire of several HA stem–binding memory B cells generated after H5N1 vaccination capable of binding both group 1 and group 2 subtypes (*24*). Three different classes of broadly neutralizing antibodies were identified in multiple donors with shared molecular characteristics and binding footprints. Although examples of antibodies with the molecular characteristics of each of these different classes had been previously reported in isolated cases (*14*, *23*, *25*), this was the first demonstration that there are common pathways across individuals to generate cross-group broadly neutralizing antibodies. This engenders hope that designing vaccine strategies capable of preferentially eliciting these classes of HA stem–specific broadly neutralizing antibodies across the human population would contribute to a universal influenza vaccine strategy.

[1]Vaccine Research Center, National Institute of Allergy and Infectious Diseases, National Institutes of Health, Bethesda, MD 20892, USA. [2]Electron Microscopy Laboratory, Cancer Research Technology Program, Leidos Biomedical Research Inc., Frederick National Laboratory for Cancer Research, Frederick, MD 21701, USA. [3]Department of Microbiology and Immunology, Peter Doherty Institute for Infection and Immunity, University of Melbourne, Melbourne, Victoria, Australia.
*Corresponding author. Email: adrian.mcdermott@nih.gov (A.B.M.); sarah.andrews2@nih.gov (S.F.A.)

Although several studies have investigated the HA stem response to group 1 subtypes, little work has been done to systematically characterize the HA stem response upon immunization with a group 2 subtype. Because of profound differences in the HA stem region between group 1 and group 2 influenza subtypes (*3*, *21*), we hypothesized that the Ig repertoire of reactive B cells would be quite different and inform strategies to elicit a broad cross-group protective B cell response. We therefore undertook a direct comparison of the HA-specific memory B cell responses to a group 1 (H5N1) versus a group 2 (H7N9) influenza subtype vaccine. Both are avian influenza viruses and generate substantial HA stem–directed responses. We found that the overall magnitude of vaccine-induced HA-binding B cells was lower after H7N9 vaccination compared with H5N1 immunization. However, H7N9 vaccination induced higher levels of HA-specific B cells broadly reactive across group 1 and group 2 HA subtypes. Given these results, group 2–based immunogens should be explored further as candidate vaccines to induce broadly protective influenza immunity.

RESULTS

Magnitude and specificity of an H5N1 versus H7N9 vaccine B cell response

To compare the HA-specific response between group 1 and group 2 influenza subtypes (Fig. 1A), we carried out in-depth analyses of the B cell responses in two phase 1 open-label randomized clinical trials in healthy adults. In the first study (VRC 310), donors were primed with A/Indonesia/05/2005 H5N1 HA DNA or matched H5N1 monovalent inactivated vaccine (MIV) followed by an MIV boost administered to different groups at intervals from 4 to 24 weeks later (hereafter termed H5N1 vaccine) (*26*). In a second study (VRC 315), donors were primed with A/Anhui/1/2013 H7N9 HA DNA, A/Shanghai/02/2013 H7N9 MIV, or both, followed by an H7N9 MIV boost 16 weeks later (hereafter termed H7N9 vaccine) (*27*). This is a homologous prime/boost because there is no difference in the HA protein between H7N9 A/Anhui/1/2013 and A/Shanghai/02/2013.

We first compared the frequency of memory B cells recognizing the HA of the vaccinating influenza strain (A/Indonesia/05/2005 H5 HA or A/Shanghai/02/13 H7 HA) at 2 weeks after MIV immunization (the peak of the memory response) by flow cytometry using HA probes (Fig. 1B) (*16*). To compare the response in donors with similar vaccination protocols, we limited the analysis to 24 donors from the VRC 310 (H5N1) trial that received an MIV or DNA prime with a 16- to 24-week prime/boost interval (groups 1, 5, and 6), which were most comparable to the VRC 315 (H7N9) trial (fig. S1, A and B). The overall frequency of vaccine-specific HA-binding IgG^+ B cells was lower after H7 vaccination compared with that after H5 vaccination (Fig. 1, B and E). On average, 1.26% of the IgG^+ B cell compartment recognized H5 HA after H5N1 vaccination, whereas a mean of 0.37% of the IgG^+ B cells bound H7 HA after H7N9 vaccination (Fig. 1E). We next wanted to determine the frequency of H5 or H7 HA–specific memory B cells that cross-reacted with another group 1 or group 2 HA antigen. To do this, we costained cells from the H5N1 vaccine trial with H5, H1, and H3 HA probes or cells from the H7N9 vaccine trial with H7, H1, and H3 HA probes (Fig. 1C). A mean of 60% of the H7 HA–specific B cells elicited by H7N9 across the donors did not cross-react with H1 or H3 HA (termed subtype-specific), whereas 45% of the H5 HA–specific B cells in the H5N1 trial donors did not cross-react with H1 or H3 HA [Fig. 1, F (left) and G]. However, of the H7N9-induced B cells that did cross-react with other subtypes, they were more broadly reactive, with ~45% of the cross-reactive H7 HA^+ cells detected after H7N9 vaccination able to bind both group 2 H3 HA and group 1 H1 HA (cross-group reactive; red) (Fig. 1G). In contrast, most (~90%) of the cross-reactive B cells detected after H5N1 vaccination only recognized H1 HA, another group 1 subtype (intragroup reactive; blue) (Fig. 1G).

Most of the broadly reactive HA-specific B cells are thought to bind to conserved regions in the HA stem. Previous work has suggested that 80 to 90% of the cross-reactive $H5H1^+$ cells in the H5N1 trial bind the HA stem (*15*). The recently described stabilized group 1 stem–only probe (*6*) (modified to be derived from A/California/04/2009 H1 HA) allowed us to directly analyze the proportion of vaccine-specific B cells from each trial that exhibited cross-group HA stem binding. Because we did not have a group 2 stem–only probe available, we looked for B cells that bound the group 1 stem–only probe and also recognized both group 1 H1 and group 2 H3 full-length HA (Fig. 1D). Expectedly, we found that though a high proportion of H5 HA^+ cells induced by H5N1 vaccination bound the H1 HA stem (Fig. 1D), only a mean of 1.5% recognized the H1 HA stem and both full-length H1 and H3 HA (Fig. 1H). In contrast, a mean of 26% of the H7 HA^+ cells elicited upon H7N9 vaccination cross-reacted with the H1 HA stem and full-length H1 and H3 HA (Fig. 1H). This difference was so remarkable that, despite the lower overall HA response, there was, on average, a significantly ($P < 0.0001$) higher number of cross-group stem-binding B cells elicited after H7N9 vaccination compared with H5N1 vaccination (Fig. 1I). We subdivided the donors into their vaccine groups based on the type of prime or prime/boost interval (fig. S1, A and B) and confirmed that this difference was independent of the vaccine regimen (fig. S1, C and D). The number of cross-reactive B cells in the IgM memory B cell compartment was negligible for both vaccine trials (fig. S1E). We conclude that the response to H5N1 is largely group 1–specific, whereas H7N9 vaccination induces higher levels of cross-group HA stem–specific B cells.

Ig repertoire of the H5N1 and H7N9 vaccine B cell response

Considering that most cross-reactive B cells generated after H5N1 vaccination displayed primarily group 1 specificity and H7N9-induced B cells displayed greater cross-group reactivity, we next analyzed the Ig repertoire of the cross-reactive memory B cells generated by each vaccine. We single cell–sorted IgG^+ B cells from 20 donors in the H7N9 vaccine trial that bound both full-length H7 and H3 HA probes ($H7H3^+$) ($n = 1069$) 2 weeks after the H7N9 MIV. These $H7H3^+$ B cells included cells that also bound the H1 HA probe. We also single cell–sorted IgG^+ B cells from 20 donors in the H5N1 trial 2 weeks after the H5N1 MIV boost that recognized the H5 and H1 HA probes ($H5H1^+$) ($n = 1456$), including cells that also bound the H3 HA probe. These donors came from all vaccine groups, were of diverse ages, and had varied levels of cross-reactive cells after vaccination (table S2 and Fig. 2, A and B).

Cross-reactive memory B cells expressed a diverse array of VH genes, but there were notable differences in the Ig repertoire of these cells after H5N1 or H7N9 vaccination. Consistent with previous reports (*5*, *12*, *15*, *16*, *18*), VH1-69 heavily dominated the repertoire of cross-reactive cells after vaccination with group 1 subtype H5N1 (fig. S2A). However, the two most common VH genes used by $H7H3^+$ B cells in the H7N9 vaccinated donors were VH1-18 and VH6-1, representing 27.5 and 8.5% of the Ig sequences, respectively (fig. S2A). The bias toward VH1-18 and VH6-1 usage was unique to cross-reactive B cells as few subtype-specific cells that recognized only H7 HA used these VH genes (fig. S2A). The difference in VH1-69 and VH1-18 distribution

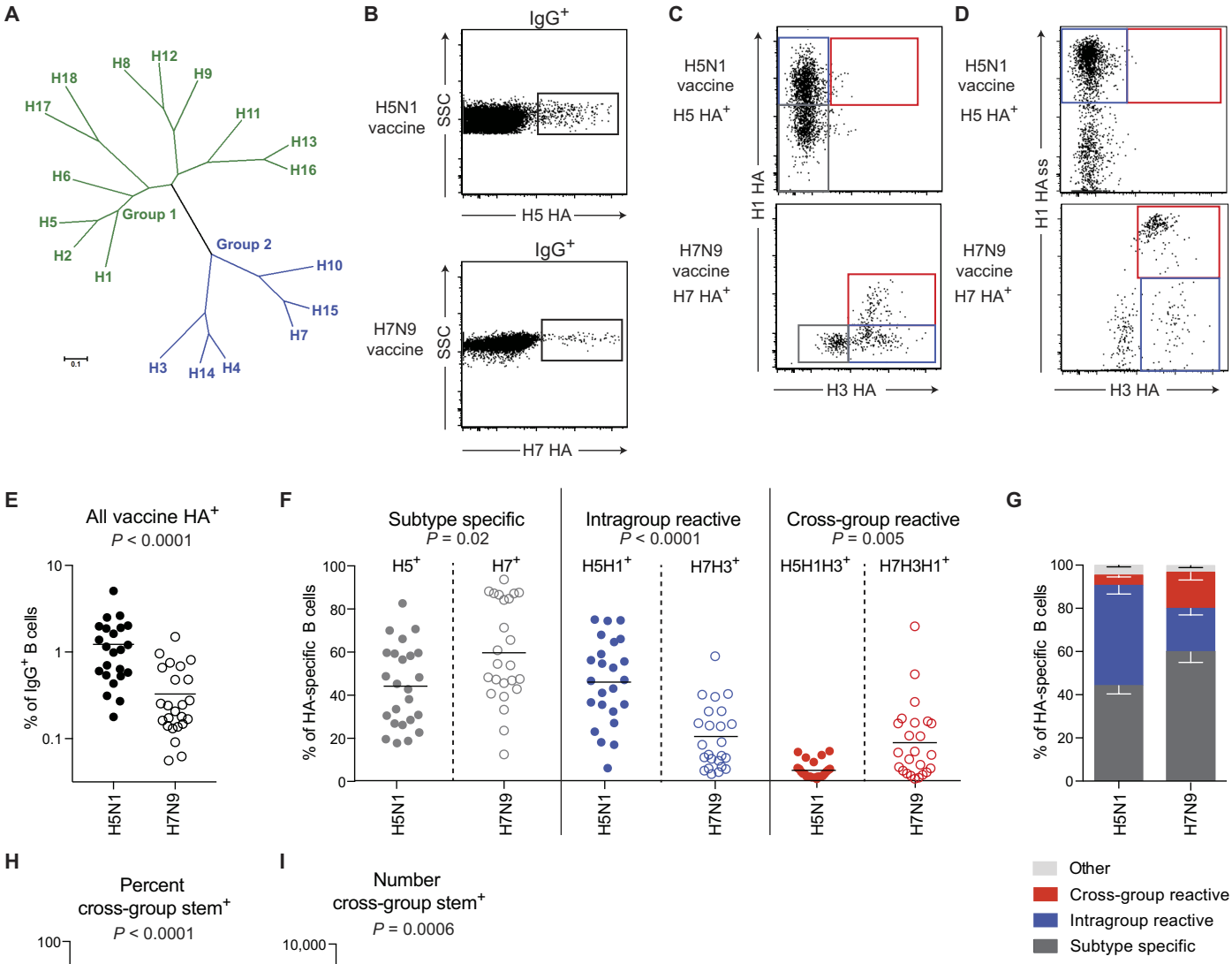

Fig. 1. Cross-reactivity of the memory IgG$^+$ B cell response to H5N1 or H7N9 vaccination. (**A**) Phylogenetic tree showing relationship of HA protein from different influenza A subtypes. HA sequences were aligned, and a maximum likelihood tree based on the amino acid sequence was produced using MEGA 7.0 (*53*). The influenza strain and respective accession numbers of each HA used are listed in table S1. (**B** to **D**) Representative flow cytometry plot of the percentage of IgG$^+$ B cells that bound full-length HA or stabilized stem of the influenza strain HA as indicated. Doublets and dead cells were excluded followed by gating on CD3$^-$CD8$^-$CD14$^-$CD56$^-$CD19$^+$ CD38^{lo} IgG$^+$ cells. Cells were further gated on H5 HA$^+$ (top) or H7 HA$^+$ (bottom) for (C) and (D). (**E**) Percentage of IgG$^+$ B cells in each donor that bound HA of the vaccinating influenza strain (H5 or H7 HA). The line indicates the mean percentage. (**F**) IgG$^+$ H5 HA$^+$ in H5N1 vaccinated volunteers and H7 HA$^+$ cells in H7N9 vaccinated volunteers were tested for the ability to bind H3 (A/Texas/50/2012) and/or H1 (A/California/04/2009) HA as shown in (C). Percentage of all H5 HA$^+$ or H7 HA$^+$ B cells, depending on the vaccine trial, that were (left) subtype-specific (H5$^+$H1$^-$H3$^-$ or H7$^+$H1$^-$H3$^-$), (middle) cross-reactive with HA from a subtype within the same group (intragroup reactive; H5$^+$H1$^+$H3$^-$ or H7$^+$H3$^+$H1$^-$), or cross-reactive with HA from subtypes across groups (cross-group reactive; H5$^+$H1$^+$H3$^+$ or H7$^+$H3$^+$H1$^+$). Each dot represents the data from one donor with the line indicating the mean. (**G**) Same data as in (F), summarized as the proportion of the total vaccinating HA response with the indicated level of cross-reactivity to influenza subtypes. The mean in each vaccine group with SEM is shown. (**H** and **I**) Percentage (H) or number per 10^6 IgG$^+$ cells (I) that bound H5 or H7 HA plus the group 1 H1 stabilized stem probe and full-length H3 and H1, as shown in (D). Data were $\log_{10}$-transformed for (E) and (I). Statistical significance was determined for all plots using unpaired nonparametric Mann-Whitney *t* test.

between H5N1 and H7N9 vaccinated groups was evident when we pooled all the sequences together in each vaccine study (Fig. 2C) or looked at the frequency of VH usage by cross-reactive B cells on a per-donor basis (Fig. 2D). VH6-1–derived transcripts were present in a small subset of donors, and expression was not statistically different between the vaccine studies on a per-donor basis (Fig. 2D). When we looked at the distribution of VH1-69, VH1-18, and VH6-1 usage between vaccine groups within each trial, we found no difference between groups, indicating

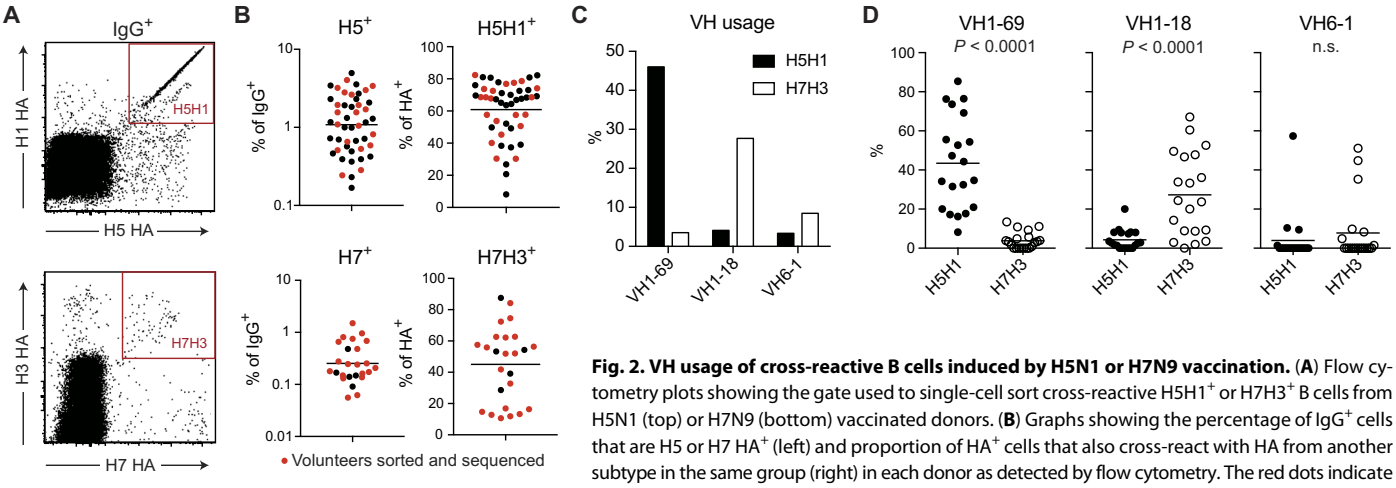

Fig. 2. VH usage of cross-reactive B cells induced by H5N1 or H7N9 vaccination. (**A**) Flow cytometry plots showing the gate used to single-cell sort cross-reactive H5H1$^+$ or H7H3$^+$ B cells from H5N1 (top) or H7N9 (bottom) vaccinated donors. (**B**) Graphs showing the percentage of IgG$^+$ cells that are H5 or H7 HA$^+$ (left) and proportion of HA$^+$ cells that also cross-react with HA from another subtype in the same group (right) in each donor as detected by flow cytometry. The red dots indicate the donors from which single-cell sorting and repertoire analysis were performed. (**C** and **D**) Comparison of percentage of Ig heavy chain sequences from all single cell–sorted H5H1$^+$ or H7H3$^+$ cells encoded by VH1-69, VH1-18, or VH6-1 genes, as indicated. In (C), the percentage of all sequences from each vaccine trial is shown. Differences in frequency for each of these three VH genes between vaccine studies were significant ($P < 0.0001$, Fisher's exact test). In (D), each dot represents the mean percentage for each donor, with the line indicating the mean for all 20 donors in each vaccine trial. *P* values were determined using unpaired nonparametric Mann-Whitney *t* test. n.s., not significant.

that the vaccine antigen, not the vaccination regimen, was responsible for the difference in repertoire that we observed (fig. S2B).

HA stem–specific B cells induced by group 1 and expressing VH1-69 rarely recognize group 2 HA subtypes (*5*, *12*, *15*, *16*, *18*). However, in our previous work, one VH6-1 and two VH1-18 (termed VH1-18 + DH3-9 and VH1-18 QXXV) multidonor Ig classes capable of binding both the group 1 and group 2 HA stem were identified in a subset of donors in the H5N1 vaccine trial (*24*). We therefore analyzed the Igs expressed by cross-reactive B cells after H7N9 or H5N1 exposure for the presence of these multidonor class signatures based on their Ig heavy chain characteristics (Fig. 3A). Eighty-three percent of the VH1-18–expressing H7H3$^+$ B cells had a VH1-18 QXXV class signature, whereas only 32% of the H5H1$^+$ B cells had this signature (Fig. 3B). Very few of the VH1-18–expressing cells isolated from either trial had a VH1-18 + DH3-9 class signature (Fig. 3B). Some subtype-specific memory B cells that recognized only H7 or H5 HA expressed VH1-18, but none had a CDRH3 that matched one of the multidonor class signatures (Fig. 3B). Most of the VH6-1 Igs expressed by cross-reactive B cells found in either vaccine trial matched the VH6-1 multidonor class signature (Fig. 3C). Overall, in 6 of 20 donors from the H5N1 vaccine trial, we detected cells expressing Igs that belonged to one of the three multidonor classes (Fig. 3E). These made up 5% of the total H5H1$^+$ B cell sequences (Fig. 3D). In contrast, we found H7H3$^+$ memory B cells expressing Igs that matched one of the multidonor classes in 17 of 20 donors, making up 29% of all sequences from cross-reactive B cells sorted after the H7N9 vaccine (Fig. 3, D and E).

Functional characteristics of multidonor classes

To verify that B cells with multidonor class sequence signatures present after H7N9 vaccination were broadly reactive across influenza A subtypes, we expressed 20 mAbs representing 20 different lineages from 11 different donors (tables S3 and S7). These 20 mAbs included a representative of eight of nine VH6-1 class lineages, all the VH1-18 + DH3-9 multidonor class lineages, and a third of the VH1-18 QXXV class lineages that we identified. We first tested the binding of these 20 mAbs against a panel of full-length HA from group 1 and group 2 strains as well as the H1 HA stem–only recombinant protein described above. All 20 mAbs bound HA from group 1 and group 2 subtypes, but the breadth of binding within each group varied between mAbs (Fig. 4A). The mAbs followed the differential binding patterns that we have previously observed between the multidonor classes (*24*), where the VH1-18 QXXV class mAbs bound preferentially to group 2 strains and the VH1-18 + DH3-9 class mAbs preferentially bound to group 1 subtypes (Fig. 4A). VH6-1 class mAbs as a whole had the greatest breadth of binding across the six subtypes tested (Fig. 4A).

When we tested the microneutralization capacity of the mAbs against the group 1 influenza strain A/California/04/2009 (H1N1) and group 2 strain A/Texas/50/2012 (H3N2), we found that despite robust binding to these two strains by all mAbs, only members of the VH6-1 class were able to neutralize both strains in this assay (Fig. 4B and table S4). VH1-18 + DH3-9 class mAbs neutralized H1N1 A/California/04/2009 but not H3N2 A/Texas/50/2012, whereas the opposite was observed with VH1-18 QXXV class mAbs (Fig. 4B and table S4). We tested the neutralization capacity of these mAbs against a panel of nine influenza strains across six subtypes using the pseudotype neutralization assay and observed similar patterns of neutralization throughout group 1 and group 2 strains for all three classes using this assay (table S5).

Antibodies not only directly prevent viral attachment or fusion and subsequent infection but also can exert protective functions through its Fc region. HA stem–specific antibodies, in particular, have been shown to protect against influenza via Fc-mediated functions (*28*, *29*). To further evaluate the protective ability of these mAbs across group 1 and group 2 strains, we tested the ability of one representative antibody from each class to protect mice infected with A/California/07/2009 (H1N1) or A/Shanghai/02/2013 (H7N9). When mAbs were given 24 hours before H7N9 infection, we observed a 90 to 100% survival in mice that received one of the multidonor class mAbs, with no loss in weight in most of the animals (Fig. 4C, top). Similarly, mAbs from each of the classes provided 100% protection from H1N1 infection in mice with minimal loss in weight (Fig. 4C, bottom). This was true even for the VH1-18 QXXV class mAb class, which showed no in vitro neutralization capacity against this influenza strain (Fig. 4B). In contrast, all but

one of the mice that received the anti-HIV mAb VRC01 had substantial weight loss after infection and were euthanized (Fig. 4C). We conclude that close to one-third of the cross-reactive B cell memory response to H7N9 vaccination in these 20 donors is composed of multidonor lineages capable of protecting against infection with both a group 1 and group 2 subtype.

Characterization of new cross-group lineages elicited by H7N9 vaccination

The VH1-18 and VH6-1 multidonor classes comprised 59% of the Ig sequences (n = 531) isolated from cross-group HA stem–binding B cells as detected by flow cytometry after H7N9 vaccination. The remaining cross-group stem-specific memory B cells expressed Igs with a diverse array of heavy and light chain variable genes. Among these sequences, we looked for the presence of new multidonor class signatures not identified previously. The Ig heavy chain from seven lineages from four different donors had an 18–amino acid CDRH3 with a common motif derived from the recombination of either VH1-2 or VH3-53 with DH3-9/DH3-3 and different JH genes (Fig. 5, A and B, and tables S3 and S7). The most conserved residues [L(Q/R)(Y/F)FDW] in the middle of the CDRH3 are encoded by the germline DH gene with somatic hypermutations primarily accounting for the variation between Ig sequences in this region (fig. S3, A and B). In six of seven lineages, the heavy chain was paired with either a VL2-8 or VL2-14 light chain (Fig. 5B). By negative-stain electron microscopy (EM), we looked at the Fab of two of the antibodies in complex with H7 HA and verified that they bind the HA stem (Fig. 5C). We also tested their ability to bind HA from multiple subtypes, and consistent with the idea that this constitutes a specific class of Igs, we found that all lineages had a very similar binding pattern across influenza subtypes (Fig. 5D). All but one antibody (04-1B12) bound group 2 H3 and H7 subtypes and a limited number of group 1 H1N1 and H9N2 influenza strains (Fig. 5D). All members of this class were able to neutralize A/Texas/50/2012 (H3N2) but were unable to neutralize A/California/04/2009 (H1N1) in a microneutralization assay (Fig. 5E and table S4). A pseudotype neutralization assay against a broader panel of influenza strains showed similar findings (table S5). However, like the multidonor classes described above, passive transfer of a mAb from this class (02-1F07) into mice followed by infection with H7N9 or H1N1 showed the ability to protect against both a group 1 and a group 2 influenza strain (Fig. 5F).

To investigate whether these VH1-2/VH3-53 lineages looked structurally similar, we produced high-resolution structures of the Fabs of one VH1-2– and two VH3-53–encoded antibodies (table S6). The antibody structures show marked similarity despite the different VH-encoding genes with an average root mean square deviation (RMSD) of <0.6 Å for the Fv domains (Fig. 5G). The CDRH3s of the antibodies display the greatest differences, but comparing all three structures, the CDRH3 C-α atoms appeared to rotate relative to each other, and each displayed a characteristic aromatic Lys/Arg at the CDRH3 apex (Fig. 5G). We conclude that these VH1-2/VH3-53 lineages constitute a distinct class of genetically similar Igs elicited in multiple donors upon H7N9 vaccination.

In addition to the multidonor class described above, we also identified two lineages with particularly broad reactivity expressed by a substantial proportion of the cross-group HA stem–binding B cells in the respective donors from which we isolated them (Fig. 6A). One lineage was encoded by VH3-48, the other used a VH3-11 Ig heavy chain, and both paired with a VK1-39–encoded light chain (Fig. 6B and tables S3 and S7). Negative-stain EM of Fabs in complex with H7 HA confirmed that representative mAbs from both lineages (13-1B02 and 53-1A09) bound the HA stem (Fig. 6C). These mAbs varied somewhat in their specificity to HA from different subtypes but were overall broadly reactive (Fig. 6D) and able to neutralize both group 1 and group 2 strains (Fig. 6E and tables S4 and S5). In addition, when we tested the ability of one of the antibodies (53-1A09) to protect against H1N1 or H7N9 infection in a mouse model, we observed 90 to 100% protection with minimal weight loss (Fig. 6F). Crystallization of Fabs from each antibody showed a high level of similarity (<0.5 Å RMSD) between these two antibodies in the VH and VK (variable kappa) region (Fig. 6G and table S6). However, analysis of the CDRH3 indicated that many equivalent residues in sequence were located >10 Å apart (Fig. 6G), suggesting that they may interact with the HA stem in different ways. In summary, H7N9 vaccination induces a diverse array of cross-reactive HA stem–binding memory B cells with common Ig genetic signatures identified in multiple donors as well as broadly binding and protective donor-specific lineages.

Memory recall and expansion of cross-group HA stem–binding B cells

Several studies have shown that HA stem–binding B cells reactive to novel influenza subtypes are preexistent in the memory repertoire and are expanded upon vaccination (*14*, *15*, *22*, *24*, *30*). Many of the $H7H3^+$ memory B cell lineages found 2 weeks after the vaccine boost were also found before H7N9 vaccination (Fig. 7A, left) and most of these lineages (30 of 36) were expanded 2 weeks after the vaccine boost (Fig. 7B). In contrast, when we searched for lineages belonging to memory B cells that bound H7 HA alone, only one lineage in a single donor was found before vaccination (Fig. 7A, right). Expectedly, the mean VH mutation level for cross-group or intragroup 2 reactive B cells was twice that of subtype-specific $H7\ HA^+$ cells (7% versus 3.6%) (Fig. 7C). Together, this demonstrates that most, if not all, of the cross-reactive response detected is a vaccine-induced expansion of a preexisting memory repertoire, presumably generated from exposure to seasonal influenza subtypes. The cross-group stem-binding B cells were also highly clonal (Fig. 7D), suggesting that most individuals have a few dominant lineages capable of cross-group stem binding.

Three of the vaccine trial volunteers described herein participated in both the H5N1 and H7N9 trials, allowing us to directly compare the repertoire of the response to both a group 1 and group 2 subtype in the same individual with a 5-year interval between the two vaccine trials. These three donors had varied responses, and we observed no difference in their B cell specificity or repertoire after H7N9 vaccination compared to other volunteers that had not received previous H5N1 influenza vaccines (fig. S4, A and B).

The H5H1 cross-reactive repertoire of the first volunteer after H5N1 vaccination was primarily composed of a group 1–only VH1-69–encoded response (Figs. 3E and 7E). However, 11% of the cross-reactive B cells were able to bind both the group 1 and group 2 HA stem and expressed Igs from two different lineages (Fig. 7E). After subsequent H7N9 immunization, almost 40% of the cross-reactive $H7H3^+$ B cells in this volunteer belonged to one of these two lineages (Fig. 7E). Both lineages expanded after H5N1 vaccination, were still detectable at low levels before H7N9 vaccination, and expanded again 2 weeks after the H7N9 vaccine boost (Fig. 7F).

The second donor had the highest level of cross-group stem-binding B cells among all 48 donors analyzed by flow cytometry in the H5N1 vaccine study (fig. S4C). In response to both H5N1 and H7N9 vaccination,

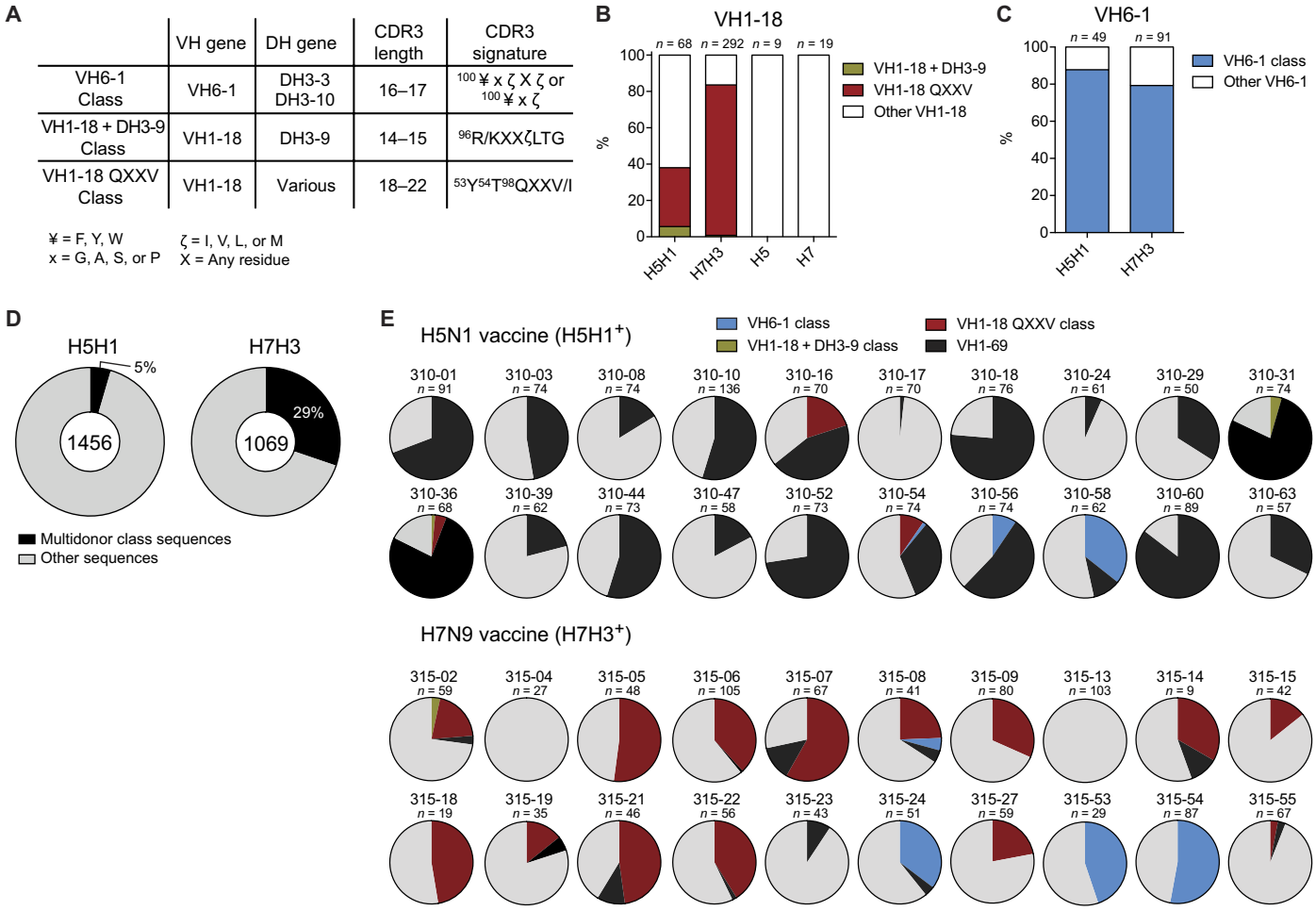

Fig. 3. Evaluation of multidonor class Ig sequences obtained from H5N1 and H7N9 vaccinated donors. (**A**) Criteria used to classify paired heavy and light chains from single cells into the three multidonor classes. (**B** and **C**) Percentage of $H5H1^+$, $H7H3^+$, $H5^+H1^-$, or $H7^+H3^-$ single cell–sorted cells that expressed a VH1-18 or VH6-1 heavy chain and had an Ig molecular signature that fit one of the three classes indicated in (A). No $H5^+H1^-$ or $H7^+H3^-$ B cells expressing VH6-1 were found. The total number of sequences analyzed in each category is indicated above the bar. (**D**) Percentage of all $H5H1^+$ or $H7H3^+$ cells whose Ig heavy chain sequence matched the molecular signature of one of the three multidonor classes. Statistical significance between the $H5H1^+$ and $H7H3^+$ cells by Fisher's exact test was $P < 0.0001$. (**E**) Each pie chart shows the proportion of $H5H1^+$ (top) or $H7H3^+$ (bottom) cross-reactive B cells in each donor that expressed an Ig heavy/light chain that matched one of the indicated multidonor classes or VH1-69. The volunteer number and total number of sequences obtained from that donor are indicated above each pie chart.

about half of the cross-reactive response bound both the group 1 and group 2 HA stem. Cross-group stem-binding B cells after H5N1 vaccination expressed Igs that were part of one of three different lineages with a VH6-1 class signature (Fig. 7G). In response to H7N9 vaccination, all of the cross-group stem-binding B cells that we sequenced belonged to two of these lineages (Fig. 7G). Similar to the previous donor, both lineages were expanded 2 weeks after H5N1 or H7N9 vaccination and contracted in between the two vaccine trials (Fig. 7H).

In the third donor, we were unable to detect cross-group HA stem–binding B cells after H5N1 vaccination (Fig. 7I). However, after H7N9 vaccination, roughly 25% of the $H7H3^+$ B cells bound group 1 and group 2 subtypes with the most prevalent lineage being the broadly neutralizing VH3-48 lineage described above (Figs. 6 and 7I). This lineage was present in the memory repertoire immediately before H7N9 vaccination, so it is unclear why this lineage was not detected after H5N1 vaccination. Group 1–specific lineages may have dominated the response after the H5N1 vaccine to such a degree that we could not detect this lineage, or, alternatively, it could have first emerged in this donor in the 5 years between the two vaccinations.

We conclude that individuals maintain low levels of circulating HA stem–specific memory B cells capable of cross-group binding. These cells can be readily expanded upon exposure to either an influenza group 1 or group 2 subtype. However, they are preferentially expanded by a group 2 influenza subtype such as H7N9.

DISCUSSION

To design an influenza vaccine capable of inducing a robust HA stem–directed response, we need to better understand the natural human immune response to this structure. Few cross-reactive B cell responses characterized to date have been in the context of immunization with a group 2 immunogen because most studies have focused on group 1–induced responses. The few previous studies looking at the B cell response to H7N9 have characterized mAbs cloned from

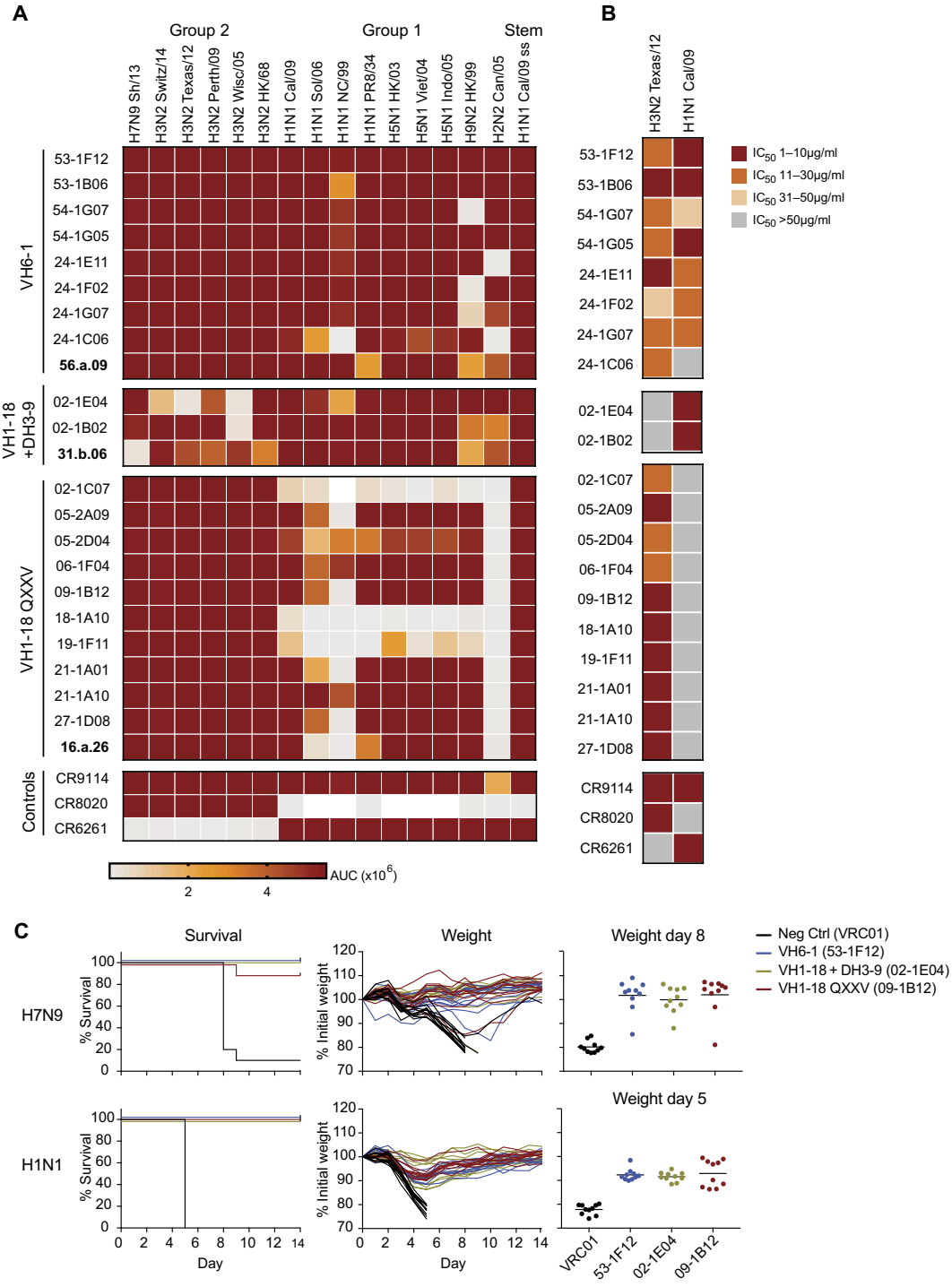

Fig. 4. Functional characterization of multidonor class antibodies. (**A** and **B**) mAbs belonging to the multidonor VH6-1, VH1-18^{+} DH3-9, and VH1-18 QXXV classes or control antibodies were tested for binding to full-length recombinant HA or the stabilized stem of the indicated influenza strains (A) or neutralization in a microneutralization assay with the indicated strains (B). Full influenza strain names are detailed in Materials and Methods. Antibodies in bold were published previously (*24*) and shown for comparison. Control antibodies were previously characterized as group 1 stem binding (CR6261) (*17*), group 2 stem binding (CR8020) (*21*), or group 1 and group 2 stem binding (CR9114) (*2*). All other antibodies were cloned from B cells isolated after H7N9 vaccination. In (A), binding of each antibody to each strain is color-coded according to the AUC of the titration curve as indicated in the color legend. In (B), the mAbs are color-coded according to the microneutralization IC_{50} for each strain, as indicated in the legend. Actual values are in table S4. Representative data are shown from at least two independent experiments. (**C**) Mice were passively administered with the indicated antibody (5 mg/kg) (10 mice per group) 24 hours before infection with A/Anhui/01/2013 (H7N9) or A/California/07/2009 (H1N1) as indicated. As a control, one group received VRC01 IgG, an HIV-specific antibody. Mice were euthanized when they reached 80% of their initial weight. The left graph shows the Kaplan-Meier survival curve. There was greater survival in all groups that received an HA stem–binding antibody ($P \leq 0.001$, Fisher's exact test) compared to the control group. The middle graph shows the percent weight loss over time with each line representing one mouse. On the right, the percent weight loss is shown for animals in each group on the last day when all animals infected with that strain had a recorded weight. The weight loss is statistically lower ($P < 0.0001$, Mann-Whitney *t* test) in all groups that received an HA stem–binding antibody compared to the control group.

B cells isolated from individuals after either a H7N9 MIV or H7N9 live attenuated cold-adapted vaccine (*31*, *32*). By screening large numbers of cells to identify a few H7 reactive B cells, these studies have demonstrated that H7N9 vaccination can elicit B cells targeting both the HA head and stem with a wide range of cross-reactivity and neutralization potential.

We undertook a direct comparison of a group 1 and a group 2 HA stem memory B cell response from two clinical trials with similar immunization protocols. Using HA probes that have the sialic acid binding site mutated to eliminate nonspecific binding, we could specifically detect and sort HA head or stem subtype–specific and cross-reactive memory B cells by flow cytometry (*6*, *16*). In this way,

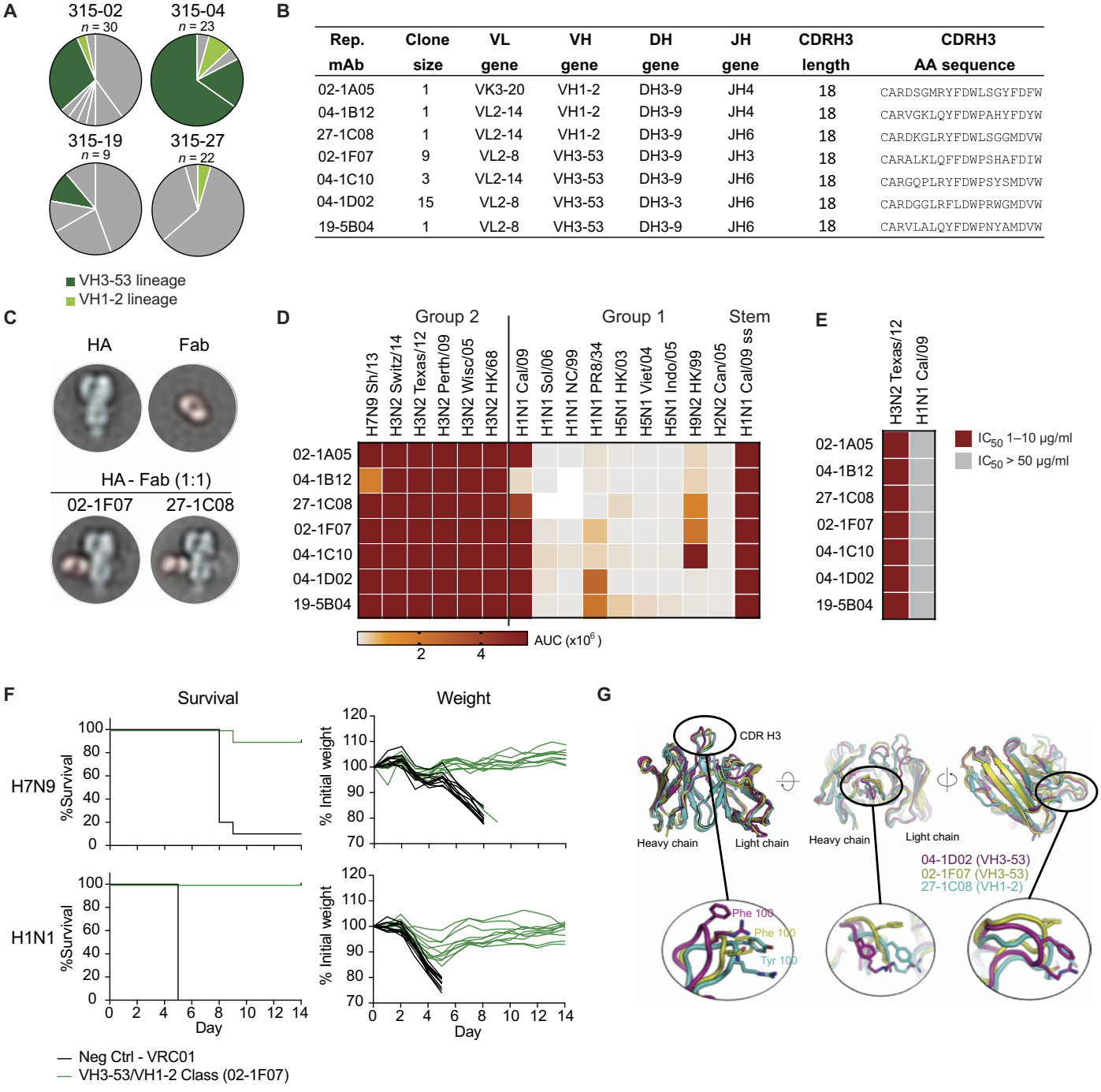

Rep. mAb	Clone size	VL gene	VH gene	DH gene	JH gene	CDRH3 length	CDRH3 AA sequence
02-1A05	1	VK3-20	VH1-2	DH3-9	JH4	18	CARDSGMRYFDWLSGYFDFW
04-1B12	1	VL2-14	VH1-2	DH3-9	JH4	18	CARVGKLQYFDWPAHYFDYW
27-1C08	1	VL2-14	VH1-2	DH3-9	JH6	18	CARDKGLRYFDWLSGGMDVW
02-1F07	9	VL2-8	VH3-53	DH3-9	JH3	18	CARALKLQFFDWPSHAFDIW
04-1C10	3	VL2-14	VH3-53	DH3-9	JH6	18	CARGQPLRYFDWPSYSMDVW
04-1D02	15	VL2-8	VH3-53	DH3-3	JH6	18	CARDGGLRFLDWPRWGMDVW
19-5B04	1	VL2-8	VH3-53	DH3-9	JH6	18	CARVLALQYFDWPNYAMDVW

Fig. 5. Characterization of a novel HA stem–binding multidonor class. (**A**) Pie charts showing proportion of sequences obtained from stem-binding B cells in four donors that expressed Igs with a canonical 18–amino acid CDRH3. Clonally related Igs are separated by white lines in each pie chart. Clones with the canonical CDRH3 motif are in green, and all other sequences are in gray. (**B**) Table showing genetic characteristics of a representative antibody from each lineage. (**C**) Negative-stain EM images of A/Shanghai/02/13 H7 HA, an antibody Fab alone, and H7 HA in complex with Fabs of indicated antibodies. (**D** and **E**) Binding AUC (D) and microneutralization IC_{50} (E) of representative mAbs as described in Fig.4. (**F**) Kaplan-Meier survival and weight loss over time of H7N9- or H1N1-infected mice 24 hours after passive transfer of 02-1F07 (5 mg/kg) as in Fig.4. (**G**) Crystal structures of three representative antibodies are overlaid with the CDRH3 loop shown in the inset panels. The overlaid structures are rotated to allow visualization of the highly similar structures as well as the protruding nature of the hydrophobic CDRH3 tip.

we were able to characterize the specificity and the Ig repertoire of thousands of memory B cells elicited by either H7N1 or H5N1 immunization at the single-cell level from 40 vaccinated donors. We found that despite a lower overall HA-specific B cell response to H7N9, the absolute number of cross-group HA stem–reactive B cells generated after H7N9 vaccination was higher. The VH repertoire of cross-reactive B cells generated after H7N9 vaccination was also much more diverse than the group 1 H5N1 response. It is well known that VH1-69

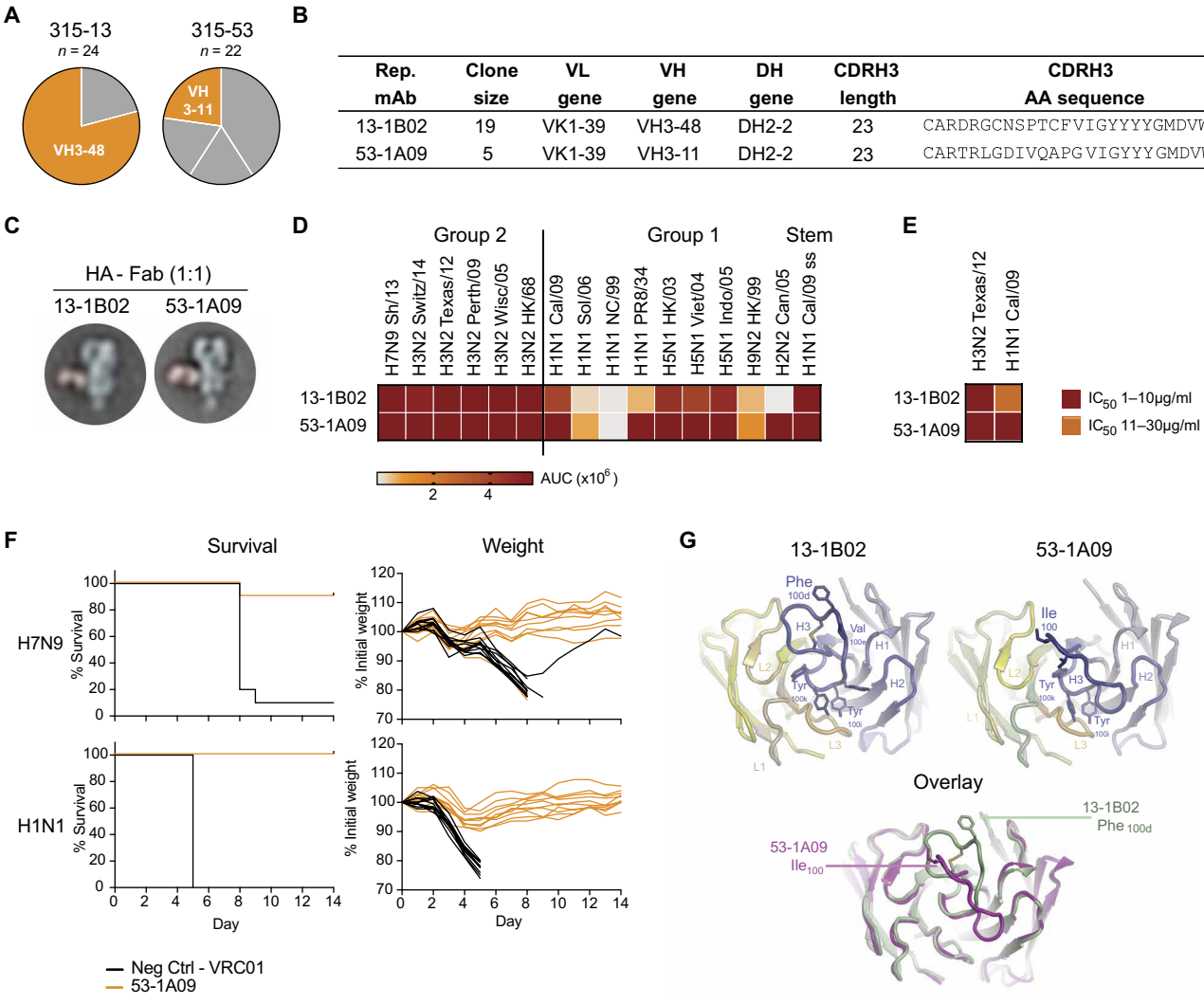

Rep. mAb	Clone size	VL gene	VH gene	DH gene	CDRH3 length	CDRH3 AA sequence
13-1B02	19	VK1-39	VH3-48	DH2-2	23	CARDRGCNSPTCFVIGYYYYGMDVW
53-1A09	5	VK1-39	VH3-11	DH2-2	23	CARTRLGDIVQAPGVIGYYYGMDVW

Fig. 6. Characterization of unique cross-group HA stem–binding lineages. (**A**) Pie charts showing proportion of volunteer-unique cross-group HA stem–binding lineages in two donors. White lines separate clonally related sequences. The lineages described here are in orange. (**B**) Table showing genetic characteristics of a representative antibody from each lineage. (**C**) Negative-stain EM images of H7 HA in complex with Fabs of indicated antibodies. (**D** and **E**) Binding AUC (D) and microneutralization IC_{50} (E) as in Fig. 4 for one representative antibody of each lineage. (**F**) Kaplan-Meier survival curves and weight loss over time of mice infected with an H7N9 or H1N1 influenza strain 24 hours after passive transfer of the 53-1A09 antibody (5 mg/kg). (**G**) Crystal structures of 13-1B02 and 53-1A09 antibodies are shown in ribbon representation with select CDRH3 residues shown in stick representation (top). CDR regions 1 to 3 for both the heavy and light chain are also indicated. Both structures reveal a protruding hydrophobic CDRH3. The two antibodies are overlaid (bottom) with the most protruding CDRH3 residue for each shown in stick representation. The disulfide bond of 13-1B02 is also shown in stick.

germline antibodies with a hydrophobic CDRH2 dominate the repertoire of B cells responding to group 1 subtypes with minimal somatic hypermutation (*18*, *19*). However, because of the presence of a glycan at $Asn38_{HA2}$, an equivalent strategy to easily generate a response to the group 2 HA stem is not present in the human repertoire. As a result, the highly variable CDRH3 along with light chain interactions are important for binding the group 2 HA stem (*1*, *21*, *23*, *24*, *33*). Structural studies of group 2 and cross-group binding antibodies to the HA stem have revealed different modes of binding, suggesting that Igs use diverse strategies to achieve cross-reactive binding within group 2 or between groups (*1*, *21*, *23*, *24*, *33*). However, in each individual, the repertoire of cross-group stem-binding B cells was quite restricted and often composed of one to three large clonal families. This is likely due to a restricted number of Ig rearrangements able to bind structurally conserved epitopes on the group 1 and group 2 HA stem. Multiple rounds of activation of these broadly reactive B cells with heterosubtypic influenza exposure may also further narrow the repertoire to a few dominant lineages. We detected expansion of the same cross-group reactive clones after H5N1 and H7N9 vaccination in donors that received both vaccines.

One-third of the Igs that we sequenced from cross-group binding B cells elicited by the H7N9 vaccine belonged to the three multidonor Ig classes identified previously in the H5N1 trial (*24*). In addition, we identified a fourth cross-reactive stem-binding class with a stereotypical CDRH3-based recognition motif. Members of this class expressed either a VH1-2 or VH3-53 heavy chain but had a common CDRH3 motif primarily encoded by the D gene (DH3-9). Future work

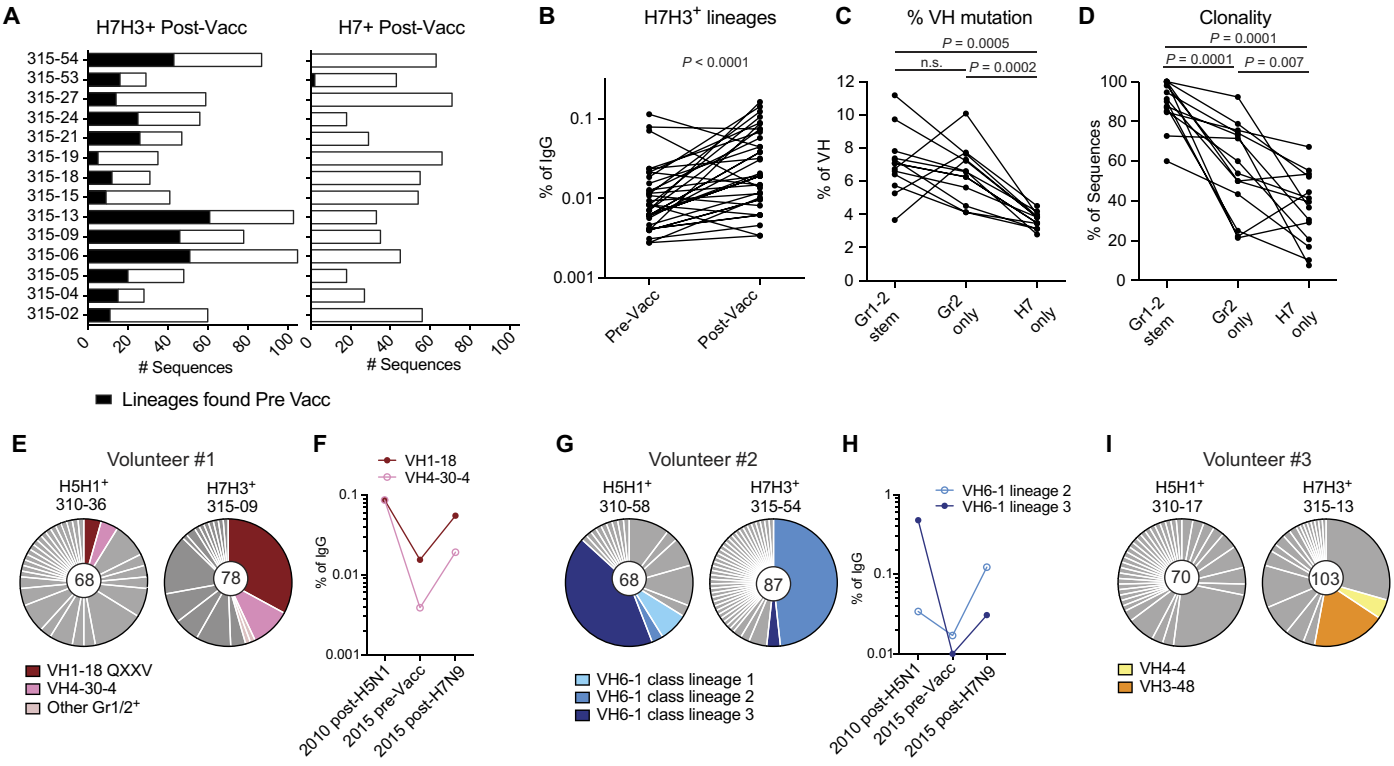

Fig. 7. Longitudinal analysis of cross-group HA stem–binding lineages. (**A**) Cells were single cell–sorted from the same donor from blood collected on the day of the H7 prime (PreVacc) and 2 weeks after the H7N9 boost (PostVacc). Each bar represents the total number of sequences from each donor amplified from cells sorted after vaccination that were H7H3$^+$ (left) or bound H7 alone (right) by flow cytometry. The sequences found after vaccination that belonged to lineages detected before vaccination as well are in black. (**B**) For each of the 36 lineages found before and after vaccination, we calculated the approximate percentage of this lineage of all IgG$^+$ cells at each time point by flow cytometry and single-cell Ig sequencing. Each line connects the proportion of a single lineage in the IgG$^+$ B cell population for each time point. Significance was determined using Wilcoxon paired nonparametric *t* test. (**C**) Mean percent mutation level of the rearranged VH gene amplified from single cell–sorted cells that were cross-group HA stem–specific (H7H3H1$^+$, Stem$^+$), group 2 only–specific (H7H3$^+$ H1$^-$), or bound H7 HA alone as indicated. Each dot connected by lines represents the mean mutation percent in each donor for each B cell specificity group. (**D**) For each donor, the percentage of Ig sequences from B cells with the indicated specificity as in (C) that were clonally related to another sequence is plotted. Statistical significance for (B) to (D) was determined using a paired nonparametric Wilcoxon *t* test. (**E**, **G**, and **I**) Pie charts showing sequences from all cross-reactive H5H1$^+$ or H7H3$^+$ B cells generated after H5N1 or H7N9 vaccination, respectively, in the same donor that received both vaccines. Individual clones are separated by white lines. Colored slices of the pie charts represent all cross-group HA stem–binding B cells as detected by flow cytometry. Representative mAbs from some of the lineages were also expressed, and cross-group binding was confirmed (Figs.4 and 6). All other cross-reactive B cells are in gray. The total number of cross-reactive B cells sorted and sequenced is indicated in the center of the chart. (**F** and **H**) Approximate percentage of each of the indicated lineages in the total IgG$^+$ population 2 weeks after the H5N1 boost, the day of the H7 vaccine prime (PreVacc), and 2 weeks after the H7N9 boost.

will further characterize contact points between this stereotypical motif and the HA stem. This class of antibodies is reminiscent of HA head receptor binding site–directed antibodies described previously that used different VH genes but with common residues in the CDRH3 mediating binding to a specific epitope on the HA head (*34*). As we accumulate data from more volunteers, other common molecular strategies by Igs to engage conserved epitopes on the HA stem may emerge.

Similar to a recent report describing an Ig lineage with this same molecular signature (*25*), B cells expressing the VH6-1 signature had a greater neutralization breadth than those with the VH1-18 QXXV signature. However, we detected the VH6-1 signature at a much lower frequency than the VH1-18 QXXV class after both H5N1 and H7N9 vaccination. Curiously, donors had responses dominated by either VH6-1 or VH1-18, not both. Of the six donors where we did not find VH1-18 QXXV Igs after H7N9 vaccination, three had robust VH6-1 encoded cross-group HA stem–binding responses. Although not conclusive, all three donors that had this strong VH6-1 response were born in the mid- to late 1960s just as a group 2 subtype (H3N2) first emerged in the human population, replacing group 1 H2N2 as the dominant subtype. Studies have suggested that the influenza subtype that one is first exposed to as an infant has a life-long effect on one's influenza-specific immune repertoire (*35*, *36*). A recent investigation that correlated incidence of H7N9 and H5N1 infection in China with birth year showed that those first exposed to group 1 H2N2 were more likely to be severely ill with group 2 H7N9 infection while protected against H5N1 and that those first exposed to group 2 H3N2 had a greater incidence of severe infection or death with group 1 H5N1 yet were protected against H7N9 (*37*). These data, along with the restricted number of broadly reactive HA-specific lineages observed in many volunteers, suggest that HA stem–specific B cell lineages are established early in life, determined in part by the subtype that an individual is first exposed to, and affect susceptibility to influenza pandemics throughout life.

Neutralizing HA stem–specific antibodies directly prevent cell infection by inhibiting membrane fusion or preventing HA cleavage (*38*). Although a few of the cross-group HA stem–binding antibodies

neutralized influenza subtypes in both groups, the neutralizing activity tended to be less broad than binding as has been shown for other stem-binding antibodies (*2*, *23*). However, there is mounting evidence that HA stem–specific antibodies can be protective independently of their neutralization capacity in vitro. All five of the cross-group stem-binding antibodies that we tested were protective against H1N1 and H7N9 infection in mice, although only two of the antibodies showed neutralization activity against both subtypes. DiLillo *et al*. tested the role for Fc-mediated mechanisms played in protection against influenza infection in vivo by broadly reactive antibodies specific for the HA stem, including antibodies belonging to the two VH1-18 multidonor classes (*28*, *29*). Through mouse in vivo protection studies with antibodies that could or could not engage the FcγR, they concluded that Fc-FcγR interactions were the primary mechanism for protection mediated by broadly reactive HA stem–binding B cells in vivo. Immunization with HA stem–only constructs in animal models also showed heterosubtypic protection that correlated with heterosubtypic serum binding titers and antibody-dependent cellular cytotoxicity (ADCC) potency but not serum neutralization titers (*6*, *7*). Fc-mediated protection seems to primarily occur with broadly specific antibodies. Non-neutralizing strain-specific antibodies have been shown to be nonprotective in vivo and fail to mediate ADCC (*29*, *31*).

In designing an immunogen that specifically elicits B cells expressing these broadly protective antibodies, both induction and boosting steps need to be considered. Antigen structure is critical for engaging germline versions of stem-binding B cells and guiding their evolution toward greater breadth. Antigen design and delivery approaches to most efficiently boost the preexisting repertoire of cross-reactive B cells to protective levels are of equal importance. Of the multidonor classes that we identified after H5N1 and H7N9 vaccination, two, including the most broadly reactive class, VH6-1, appear to be first activated by a group 1 immunogen (*24*, *25*). On the other hand, the most prevalent VH1-18 QXXV and the VH1-2/VH3-53 classes appear to be better induced by group 2 immunogens and later gain cross-reactivity to group 1 subtypes (*24*). This suggests that both group 1 and group 2 subtypes could potentially serve as the starting point for developing these multidonor broadly binding Ig classes. However, the results from the H7N9 vaccine trial described herein indicate that multidonor cross-group binding antibodies are preferentially boosted and expanded by group 2–derived antigens.

Although the difference in B cell repertoire that we observed between the two vaccine trials was quite robust, these human vaccine studies were composed of relatively few volunteers, all living within the United States and conducted 5 years apart. To further substantiate that group 2 subtypes universally elicit a broader response than group 1 subtypes in adults, these studies will need to be conducted with larger cohorts from diverse areas of the world with different influenza exposure histories. Defining whether initial priming with group 1 or group 2 antigens is more effective for eliciting cross-group antibody lineages will need to include clinical evaluation of vaccine antigens in young, influenza-naïve children. Large epidemiological studies tracing influenza exposure with repertoire and experimental clinical vaccine trials will continue to shed light on the best strategy for developing an HA stem–based universal influenza vaccine.

MATERIALS AND METHODS

Vaccine study design

The H5N1 vaccine study (VRC 310; ClinicalTrials.gov identifier NCT01086657) has been described extensively elsewhere (*26*, *39*). Like the H5N1 study, the H7N9 study (VRC 315; ClincialTrials.gov identifier NCT02206464) is a phase 1 open-label randomized clinical trial in healthy adults ages 18 to 60 years, designed to study the safety, tolerability, and immunogenicity of prime-boost vaccination regimens against H7N9 influenza (*27*). Informed consent was obtained from every enrolled volunteer. A total of 30 volunteers were enrolled and divided into three groups. One group was primed with a recombinant DNA plasmid (VRC-FLUDNA071-00-VP) that encodes for A/Anhui/1/2013 H7 HA, one group was primed with a monovalent influenza subunit virion A/Shanghai/02/2013 H7N9 vaccine (MIV) manufactured by Sanofi Pasteur Inc (Swiftwater, PA), and one group was primed with both vaccines. All groups were boosted with the MIV 16 weeks later. The 24 volunteers that completed the blood draw at 2 weeks after boost were included in this study.

Flow cytometry and single-cell sorting

Cryopreserved peripheral blood mononuclear cells from blood collected before vaccination or 2 weeks after boost from trial volunteers were stained with the anti-human mAbs CD3, CD56, CD14, CD27, and CD38 from BioLegend; IgG and IgM were from BD Biosciences; and CD19 was from Beckman Coulter. The gating strategy is shown in fig. S5. HA probes were expressed, biotinylated, and labeled with fluorochromes, as described previously (*16*). Aqua dead cell stain was added for live/dead discrimination (Thermo Fisher Scientific). Stained samples were run on an LSR II (BD Biosciences), and data were analyzed using FlowJo (TreeStar). To single-cell sort, HA-specific B cells were stained as above, and $CD19^+$ IgG^+ HA^+ B cells were single cell–sorted into 96-well plates using a FACSAria II (BD Biosciences). Addition of multiple HA probes and index sorting were used to determine the binding of each sorted B cell to HA of multiple subtypes simultaneously.

Single-cell Ig amplification and cloning

Reverse transcription was performed on sorted cells, and multiplexed polymerase chain reaction (PCR) was used to amplify Ig heavy and light chain genes, as described previously (*40*). We obtained paired heavy and light chain Ig sequences from an average of 70% of single cells on which we performed PCR. PCR products were sequenced by Beckman Coulter or Genewiz and analyzed using IMGT (*41*). Clonality was determined by paired heavy and light chain V(D)J gene usage, as well as CDR3 length and amino acid similarity.

Heavy and light chain sequences were synthesized and cloned by GenScript into IgG1, kappa, or lambda expression vectors. To produce antibodies recombinantly, Expi293 cells were transfected with plasmids encoding Ig heavy and light chain pairs with ExpiFectamine (Thermo Fisher Scientific). mAbs were purified from the cell supernatant using Sepharose Protein A (Pierce).

Mouse protection studies

All animal studies were conducted according to the National Institutes of Health (NIH) *Guide for the Care and Use of Laboratory Animals* and approved by the NIH Vaccine Research Center Animal Care and Use Committee and performed in ABSL-2 or ABSL-3 facilities at BioQual Inc. (Rockville, MD). Groups of 10 BALB/c mice (5 to 9 weeks old, female; Envigo) were given a purified monoclonal IgG antibody (5 mg/kg) intraperitoneally. Twenty-four hours later, they were anesthetized and infected intranasally with 10 LD_{50} (median lethal dose) of A/California/07/2009 (H1N1) or 25 LD_{50} of H7N9 A/Anhui/01/2013 (H7N9). The animals were monitored twice daily for development of clinical signs

and weighed daily for 14 days. Any animals that had lost 20% or more of their initial body weight were euthanized.

Microneutralization

A/California/04/2009 (H1N1) influenza virus was obtained from the Division of Viral Products, U.S. Food and Drug Administration (FDA) and expanded in MDCK (Madin-Darby canine kidney) cells. A/Texas/50/2012 (H3N2) was made by reverse genetics using the A/WSN/1933 (H1N1) backbone with HA and neuraminidase segments replaced (*42*) and expanded in MDCK-SIAT1 cells. Both viruses were expanded in the presence of tosyl phenylalanyl chloromethyl ketone (TPCK)–treated trypsin (1 μg ml^{-1}; Sigma) and titrated in MDCK or MDCK-SIAT1 cells, as described elsewhere (*43*). Briefly, DMEM (Dulbecco's modified Eagle's medium)–TPCK (DMEM with 1 μg ml^{-1} TPCK-trypsin and penicillin/streptomycin) was used to make fourfold serial dilutions of mAbs (starting at 100 μg ml^{-1}) and to dilute influenza viruses to a final concentration of 100 $TCID_{50}$ (median tissue culture infective dose) per well. In a 96-well plate, equal volumes of diluted antibody and virus were mixed and incubated for 1 hour at 37°C before adding to substrate cells. Control wells of virus alone (VC) and diluent alone (CC) were included on each plate. Cells were seeded at 1.5×10^4 cells per well 24 hours before the assays and washed once with phosphate-buffered saline (PBS) before use. Fifty microliters of antibody/virus mixture was then added to wells of prewashed cells in duplicate, and the plates were incubated for 18 or 44 hours at 37°C and 5% CO_2 humidified atmosphere for H1N1 or H3N2 virus, respectively. The cells were then fixed with 80% cold acetone and allowed to air-dry. The presence of viral nucleoprotein (NP) was detected by enzyme-linked immunosorbent assay with biotin-conjugated anti-influenza antibodies to the influenza A NPs with antibodies (MAB8257B and MAB8258B; EMD Millipore). NP staining was detected with horseradish peroxidase–conjugated streptavidin and SureBlue TMB Microwell Peroxidase Substrate (KPL). Absorbance was read at 450 nm (A_{450}) and 650 nm (A_{650}) with the SpectraMax Paradigm microplate reader (Molecular Devices). The A_{650} was used to subtract plate background. The percent neutralization was calculated setting the VC control as 0% and the CC control as 100% and plotting against antibody concentration. A curve fit was generated by a four-parameter nonlinear fit model in Prism 7 (GraphPad Software). The half-maximal inhibitory concentration (IC_{50}) of each antibody was obtained from the fitted curves.

Negative-stain EM and single-particle analysis

Complexes made by combining mAb Fabs and H7 A/Shanghai/02/2013 HA were diluted to about 0.015 mg/ml, adsorbed to freshly glow-discharged carbon film grids, washed with a buffer containing 10 mM Hepes (pH 7) and 150 mM NaCl, and stained with 0.7% uranyl formate. Images were collected semiautomatically with SerialEM (*44*) on an FEI Tecnai T20 microscope operating at 200 kV and equipped with a 2000 × 2000 Eagle charge-coupled device camera at a pixel size of 0.22 nm per pixel and a nominal magnification of 100,000. Particles were picked automatically and manually using e2boxer from the EMAN2 software package (*45*). Reference-free two-dimensional classification was performed with Relion 1.4 (*46*).

HA antibody binding assay

Meso Scale Discovery (MSD) 384-well Streptavidin-coated SECTOR Imager 2400 Reader Plates were blocked with 5% MSD blocker A for 30 to 60 min, then washed six times with the wash buffer (PBS + 0.05% Tween). The plates were then coated with biotinylated HA protein (same protein as was used for flow cytometry) for 1 hour and washed. mAbs were diluted in 1% MSD blocker A to 5 μg/ml, serially diluted threefold, and added to the coated plates. After 1 hour of incubation, plates were washed and incubated with SULFO-TAG–conjugated anti-human IgG for 1 hour. After washing, the plates were read using 1× MSD Read Buffer using an MSD SECTOR Imager 2400. Binding curves were plotted, and the area under the curve (AUC) was determined using Prism 7. HA from the following strains were tested: H7N9 A/Shanghai/02/2013, H3N2 A/Switzerland/9715293/2013, H3N2 A/Texas/50/2012, H3N2 A/Perth/16/2009, H3N2 A/Wisconsin/67/2005, H3N2 A/Hongkong/1/1968, H1N1 A/California/04/2009, H1N1 A/Solomon Islands/3/2006, H1N1 A/New Caledonia/20/1999, H1N1 A/Puerto Rico/8/1934, H5N1 A/HongKong/213/2003, H5N1 A/Vietnam/1194/2004, H5N1 A/Indonesia/05/2005, H9N2 A/Hong kong/1073/1999, and H2N2 A/Canada/720/2005.

Pseudotype neutralization assay

Influenza HA-NA pseudotyped lentiviruses that harbor a luciferase reporter gene were produced, as described previously (*47*, *48*). Pseudovirus was produced by transfection of 293T cells of HA and corresponding NA along with the lentiviral packaging and reporter plasmids. For the H1N1, H2N2, H3N2, H7N9, and H9N2 pseudovirus, a human type II transmembrane serine protease TMPRSS2 gene was cotransfected as well for proteolytic activation of HA. Forty-eight hours after transfection, supernatants were harvested, filtered, and frozen.

Neutralization assays were performed as described previously (*24*). Briefly, pseudovirus was mixed with various dilutions of mAbs for 45 min followed by addition to 293A cells in 96-well plates. Three days after infection, cells were lysed and luciferase assay reagent was added to measure luciferase activity. The following pseudoviruses were tested: H7N9 A/Anhui/01/13, H3N2 A/Texas/50/2012, H3N2 A/Hongkong/1/1968, H1N1 A/California/04/2009, H1N1 A/Solomon Islands/3/2006, H5N1 A/Vietnam/1194/2004, H5N1 A/Indonesia/5/2005, H9N2 A/Hongkong/1073/1999, and H2N2 A/Canada/720/2005.

X-ray crystallography and structural analyses

Fabs of representative mAbs were generated by digestion of antibodies with Lys-C at a 1:1000 (w/w) ratio for 3 to 4 hours at 37°C. The digestion reaction was then passed over a Protein A or Protein G column to remove the Fc fragments. The flow-through and PBS wash were pooled and concentrated to ~8 mg/ml, and 768 crystallization conditions were screened in 192-well plates (Corning) using a mosquito crystallization robot with conditions showing crystal growth further optimized by hand. Crystallographic diffraction data were collected at the Advanced Photon Source (Argonne National Laboratory) SER-CAT ID-22 or BM-22 beamline, at a wavelength of 1.00 Å and at a temperature of 100 K, and processed with HKL2000 (*49*). Iterative cycles of model building and refinement were carried out using COOT (*50*) and PHENIX (*51*) software packages, respectively, with 5% of the data acting as an R-free cross validation test set. All structural images were generated in PyMOL Molecular Graphics System, Schrodinger LLC, or UCSF Chimera (*52*).

SUPPLEMENTARY MATERIALS

immunology.sciencemag.org/cgi/content/full/2/13/eaan2676/DC1

Fig. S1. Immunization protocols and response.

Fig. S2. Ig repertoire analysis of heterosubtypic B cells.

Fig. S3. Analysis of Ig heavy chain junction of VH1-2/VH3-53 class antibodies.

Fig. S4. B cell response of volunteers that received both the H5N1 and H7N9 vaccine.

Fig. S5. Gating strategy for analyzing and sorting HA-specific B cells by flow cytometry.
Table S1. List of influenza strain HA proteins.
Table S2. Demographic information for donors used for single-cell sorting and Ig sequencing.
Table S3. Genetic characteristics of Ig heavy and light chains of expressed and characterized mAbs.
Table S4. IC_{50} microneutralization titers.
Table S5. IC_{80} neutralization titers by pseudovirus entry inhibition assay.
Table S6. Crystallographic data collection and refinement statistics.
Table S7. Ig sequences of cross-group HA-specific antibodies.
Raw data for Figs.1, 2, and 7 and figs. S1 and S2

REFERENCES AND NOTES

1. D. Corti, J. Voss, S. J. Gamblin, G. Codoni, A. Macagno, D. Jarrossay, S. G. Vachieri, D. Pinna, A. Minola, F. Vanzetta, C. Silacci, B. M. Fernandez-Rodriguez, G. Agatic, S. Bianchi, I. Giacchetto-Sasselli, L. Calder, F. Sallusto, P. Collins, L. F. Haire, N. Temperton, J. P. M. Langedijk, J. J. Skehel, A. Lanzavecchia, A neutralizing antibody selected from plasma cells that binds to group 1 and group 2 influenza A hemagglutinins. *Science* **333**, 850–856 (2011).
2. C. Dreyfus, N. S. Laursen, T. Kwaks, D. Zuijdgeest, R. Khayat, D. C. Ekiert, J. H. Lee, Z. Metlagel, M. V. Bujny, M. Jongeneelen, R. van der Vlugt, M. Lamrani, H. J. W. M. Korse, E. Geelen, Ö. Sahin, M. Sieuwerts, J. P. J. Brakenhoff, R. Vogels, O. T. W. Li, L. L. M. Poon, M. Peiris, W. Koudstaal, A. B. Ward, I. A. Wilson, J. Goudsmit, R. H. E. Friesen, Highly conserved protective epitopes on influenza B viruses. *Science* **337**, 1343–1348 (2012).
3. M. Throsby, E. van den Brink, M. Jongeneelen, L. L. M. Poon, P. Alard, L. Cornelissen, A. Bakker, F. Cox, E. van Deventer, Y. Guan, J. Cinatl, J. ter Meulen, I. Lasters, R. Carsetti, M. Peiris, J. de Kruif, J. Goudsmit, Heterosubtypic neutralizing monoclonal antibodies cross-protective against H5N1 and H1N1 recovered from human IgM^+ memory B cells. *PLOS ONE* **3**, e3942 (2008).
4. Y. Okuno, Y. Isegawa, F. Sasao, S. Ueda, A common neutralizing epitope conserved between the hemagglutinins of influenza A virus H1 and H2 strains. *J. Virol.* **67**, 2552–2558 (1993).
5. J. Sui, W. C. Hwang, S. Perez, G. Wei, D. Aird, L.-m. Chen, E. Santelli, B. Stec, G. Cadwell, M. Ali, H. Wan, A. Murakami, A. Yammanuru, T. Han, N. J. Cox, L. A. Bankston, R. O. Donis, R. C. Liddington, W. A. Marasco, Structural and functional bases for broad-spectrum neutralization of avian and human influenza A viruses. *Nat. Struct. Mol. Biol.* **16**, 265–273 (2009).
6. H. M. Yassine, J. C. Boyington, P. M. McTamney, C.-J. Wei, M. Kanekiyo, W.-P. Kong, J. R. Gallagher, L. Wang, Y. Zhang, M. G. Joyce, D. Lingwood, S. M. Moin, H. Andersen, Y. Okuno, S. S. Rao, A. K. Harris, P. D. Kwong, J. R. Mascola, G. J. Nabel, B. S. Graham, Hemagglutinin-stem nanoparticles generate heterosubtypic influenza protection. *Nat. Med.* **21**, 1065–1070 (2015).
7. A. Impagliazzo, F. Milder, H. Kuipers, M. V. Wagner, X. Zhu, R. M. B. Hoffman, R. van Meersbergen, J. Huizingh, P. Wanningen, J. Verspuij, M. de Man, Z. Ding, A. Apetri, B. Kükrer, E. Sneekes-Vriese, D. Tomkiewicz, N. S. Laursen, P. S. Lee, A. Zakrzewska, L. Dekking, J. Tolboom, L. Tettero, S. van Meerten, W. Yu, W. Koudstaal, J. Goudsmit, A. B. Ward, W. Meijberg, I. A. Wilson, K. Radošević, A stable trimeric influenza hemagglutinin stem as a broadly protective immunogen. *Science* **349**, 1301–1306 (2015).
8. T. J. Wohlbold, R. Nachbagauer, I. Margine, G. S. Tan, A. Hirsh, F. Krammer, Vaccination with soluble headless hemagglutinin protects mice from challenge with divergent influenza viruses. *Vaccine* **33**, 3314–3321 (2015).
9. R. Nachbagauer, M. S. Miller, R. Hai, A. B. Ryder, J. K. Rose, P. Palese, A. García-Sastre, F. Krammer, R. A. Albrecht, Hemagglutinin stalk immunity reduces influenza virus replication and transmission in ferrets. *J. Virol.* **90**, 3268–3273 (2016).
10. M. Klausberger, R. Tscheliessnig, S. Neff, R. Nachbagauer, T. J. Wohlbold, M. Wilde, D. Palmberger, F. Krammer, A. Jungbauer, R. Grabherr, Globular head-displayed conserved influenza H1 hemagglutinin stalk epitopes confer protection against heterologous H1N1 virus. *PLOS ONE* **11**, e0153579 (2016).
11. S. A. Valkenburg, V. V. A. Mallajosyula, O. T. W. Li, A. W. H. Chin, G. Carnell, N. Temperton, R. Varadarajan, L. L. M. Poon, Stalking influenza by vaccination with pre-fusion headless HA mini-stem. *Sci. Rep.* **6**, 22666 (2016).
12. J. Wrammert, D. Koutsonanos, G.-M. Li, S. Edupuganti, J. Sui, M. Morrissey, M. McCausland, I. Skountzou, M. Hornig, W. I. Lipkin, A. Mehta, B. Razavi, C. Del Rio, N.-Y. Zheng, J.-H. Lee, M. Huang, Z. Ali, K. Kaur, S. Andrews, R. R. Amara, Y. Wang, S. R. Das, C. D. O'Donnell, J. W. Yewdell, K. Subbarao, W. A. Marasco, M. J. Mulligan, R. Compans, R. Ahmed, P. C. Wilson, Broadly cross-reactive antibodies dominate the human B cell response against 2009 pandemic H1N1 influenza virus infection. *J. Exp. Med.* **208**, 181–193 (2011).
13. C. A. Thomson, Y. Wang, L. M. Jackson, M. Olson, W. Wang, A. Liavonchanka, L. Keleta, V. Silva, S. Diederich, R. B. Jones, J. Gubbay, J. Pasick, M. Petric, F. Jean, V. G. Allen, E. G. Brown, J. M. Rini, J. W. Schrader, Pandemic H1N1 influenza infection and vaccination in humans induces cross-protective antibodies that target the hemagglutinin stem. *Front. Immunol.* **3**, 87 (2012).
14. G.-M. Li, C. Chiu, J. Wrammert, M. McCausland, S. F. Andrews, N.-Y. Zheng, J.-H. Lee, M. Huang, X. Qu, S. Edupuganti, M. Mulligan, S. R. Das, J. W. Yewdell, A. K. Mehta, P. C. Wilson, R. Ahmed, Pandemic H1N1 influenza vaccine induces a recall response in humans that favors broadly cross-reactive memory B cells. *Proc. Natl. Acad. Sci. U.S.A.* **109**, 9047–9052 (2012).
15. A. K. Wheatley, J. R. R. Whittle, D. Lingwood, M. Kanekiyo, H. M. Yassine, S. S. Ma, S. R. Narpala, M. S. Prabhakaran, R. A. Matus-Nicodemos, R. T. Bailer, G. J. Nabel, B. S. Graham, J. E. Ledgerwood, R. A. Koup, A. B. McDermott, H5N1 vaccine-elicited memory B cells are genetically constrained by the IGHV locus in the recognition of a neutralizing epitope in the hemagglutinin stem. *J. Immunol.* **195**, 602–610 (2015).
16. J. R. R. Whittle, A. K. Wheatley, L. Wu, D. Lingwood, M. Kanekiyo, S. S. Ma, S. R. Narpala, H. M. Yassine, G. M. Frank, J. W. Yewdell, J. E. Ledgerwood, C.-J. Wei, A. B. McDermott, B. S. Graham, R. A. Koup, G. J. Nabel, Flow cytometry reveals that H5N1 vaccination elicits cross-reactive stem-directed antibodies from multiple Ig heavy-chain lineages. *J. Virol.* **88**, 4047–4057 (2014).
17. D. C. Ekiert, G. Bhabha, M.-A. Elsliger, R. H. E. Friesen, M. Jongeneelen, M. Throsby, J. Goudsmit, I. A. Wilson, Antibody recognition of a highly conserved influenza virus epitope. *Science* **324**, 246–251 (2009).
18. L. Pappas, M. Foglierini, L. Piccoli, N. L. Kallewaard, F. Turrini, C. Silacci, B. Fernandez-Rodriguez, G. Agatic, I. Giacchetto-Sasselli, G. Pellicciotta, F. Sallusto, Q. Zhu, E. Vicenzi, D. Corti, A. Lanzavecchia, Rapid development of broadly influenza neutralizing antibodies through redundant mutations. *Nature* **516**, 418–422 (2014).
19. D. Lingwood, P. M. McTamney, H. M. Yassine, J. R. R. Whittle, X. Guo, J. C. Boyington, C.-J. Wei, G. J. Nabel, Structural and genetic basis for development of broadly neutralizing influenza antibodies. *Nature* **489**, 566–570 (2012).
20. Y. Avnir, A. S. Tallarico, Q. Zhu, A. S. Bennett, G. Connelly, J. Sheehan, J. Sui, A. Fahmy, C.-y. Huang, G. Cadwell, L. A. Bankston, A. T. McGuire, L. Stamatatos, G. Wagner, R. C. Liddington, W. A. Marasco, Molecular signatures of hemagglutinin stem-directed heterosubtypic human neutralizing antibodies against influenza A viruses. *PLOS Pathog.* **10**, e1004103 (2014).
21. D. C. Ekiert, R. H. E. Friesen, G. Bhabha, T. Kwaks, M. Jongeneelen, W. Yu, C. Ophorst, F. Cox, H. J. W. M. Korse, B. Brandenburg, R. Vogels, J. P. J. Brakenhoff, R. Kompier, M. H. Koldijk, L. A. H. M. Cornelissen, L. L. M. Poon, M. Peiris, W. Koudstaal, I. A. Wilson, J. Goudsmit, A highly conserved neutralizing epitope on group 2 influenza A viruses. *Science* **333**, 843–850 (2011).
22. C. J. Henry Dunand, P. E. Leon, K. Kaur, G. S. Tan, N.-Y. Zheng, S. Andrews, M. Huang, X. Qu, Y. Huang, M. Salgado-Ferrer, I. Y. Ho, W. Taylor, R. Hai, J. Wrammert, R. Ahmed, A. García-Sastre, P. Palese, F. Krammer, P. C. Wilson, Preexisting human antibodies neutralize recently emerged H7N9 influenza strains. *J. Clin. Invest.* **125**, 1255–1268 (2015).
23. Y. Wu, M. Cho, D. Shore, M. Song, J. Choi, T. Jiang, Y.-Q. Deng, M. Bourgeois, L. Almli, H. Yang, L.-M. Chen, Y. Shi, J. Qi, A. Li, K. S. Yi, M. Chang, J. S. Bae, H. Lee, J. Shin, J. Stevens, S. Hong, C.-F. Qin, G. F. Gao, S. J. Chang, R. O. Donis, A potent broad-spectrum protective human monoclonal antibody crosslinking two haemagglutinin monomers of influenza A virus. *Nat. Commun.* **6**, 7708 (2015).
24. M. G. Joyce, A. K. Wheatley, P. V. Thomas, G.-Y. Chuang, C. Soto, R. T. Bailer, A. Druz, I. S. Georgiev, R. A. Gillespie, M. Kanekiyo, W.-P. Kong, K. Leung, S. N. Narpala, M. S. Prabhakaran, E. S. Yang, B. Zhang, Y. Zhang, M. Asokan, J. C. Boyington, T. Bylund, S. Darko, C. R. Lees, A. Ransier, C.-H. Shen, L. Wang, J. R. Whittle, X. Wu, H. M. Yassine, C. Santos, Y. Matsuoka, Y. Tsybovsky, U. Baxa; NISC Comparative Sequencing Program, J. C. Mullikin, K. Subbarao, D. C. Douek, B. S. Graham, R. A. Koup, J. E. Ledgerwood, M. Roederer, L. Shapiro, P. D. Kwong, J. R. Mascola, A. B. McDermott, Vaccine-induced antibodies that neutralize group 1 and group 2 influenza A viruses. *Cell* **166**, 609–623 (2016).
25. N. L. Kallewaard, D. Corti, P. J. Collins, U. Neu, J. M. McAuliffe, E. Benjamin, L. Wachter-Rosati, F. J. Palmer-Hill, A. Q. Yuan, P. A. Walker, M. K. Vorlaender, S. Bianchi, B. Guarino, A. De Marco, F. Vanzetta, G. Agatic, M. Foglierini, D. Pinna, B. Fernandez-Rodriguez, A. Fruehwirth, C. Silacci, R. W. Ogrodowicz, S. R. Martin, F. Sallusto, J. A. Suzich, A. Lanzavecchia, Q. Zhu, S. J. Gamblin, J. J. Skehel, Structure and function analysis of an antibody recognizing all influenza A subtypes. *Cell* **166**, 596–608 (2016).
26. J. E. Ledgerwood, K. Zephir, Z. Hu, C.-J. Wei, L. Chang, M. E. Enama, C. S. Hendel, S. Sitar, R. T. Bailer, R. A. Koup, J. R. Mascola, G. J. Nabel, B. S. Graham; VRC 310 Study Team, Prime-boost interval matters: A randomized phase 1 study to identify the minimum interval necessary to observe the H5 DNA influenza vaccine priming effect. *J. Infect. Dis.* **208**, 418–422 (2013).
27. A. D. DeZure, E. E. Coates, Z. Hu, G. V. Yamshchikov, K. L. Zephir, M. E. Enama, S. H. Plummer, I. J. Gordon, F. Kaltovich, S. Andrews, A. McDermott, M. C. Crank,

R. A. Koup, R. M. Schwartz, R. T. Bailer, X. Sun, J. R. Mascola, T. M. Tumpey, B. S. Graham, J. E. Ledgerwood, An avian influenza H7 DNA priming vaccine is safe and immunogenic in a randomized phase I clinical trial. *npj Vaccines* **2**, 15 (2017).
28. D. J. DiLillo, G. S. Tan, P. Palese, J. V. Ravetch, Broadly neutralizing hemagglutinin stalk–specific antibodies require FcγR interactions for protection against influenza virus in vivo. *Nat. Med.* **20**, 143–151 (2014).
29. D. J. DiLillo, P. Palese, P. C. Wilson, J. V. Ravetch, Broadly neutralizing anti-influenza antibodies require Fc receptor engagement for in vivo protection. *J. Clin. Invest.* **126**, 605–610 (2016).
30. S. F. Andrews, Y. Huang, K. Kaur, L. I. Popova, I. Y. Ho, N. T. Pauli, C. J. Henry Dunand, W. M. Taylor, S. Lim, M. Huang, X. Qu, J.-H. Lee, M. Salgado-Ferrer, F. Krammer, P. Palese, J. Wrammert, R. Ahmed, P. C. Wilson, Immune history profoundly affects broadly protective B cell responses to influenza. *Sci. Transl. Med.* **7**, 316ra192 (2015).
31. C. J. Henry Dunand, P. E. Leon, M. Huang, A. Choi, V. Chromikova, I. Y. Ho, G. S. Tan, J. Cruz, A. Hirsh, N.-Y. Zheng, C. E. Mullarkey, F. A. Ennis, M. Terajima, J. J. Treanor, D. J. Topham, K. Subbarao, P. Palese, F. Krammer, P. C. Wilson, Both neutralizing and non-neutralizing human H7N9 influenza vaccine-induced monoclonal antibodies confer protection. *Cell Host Microbe* **19**, 800–813 (2016).
32. N. J. Thornburg, H. Zhang, S. Bangaru, G. Sapparapu, N. Kose, R. M. Lampley, R. G. Bombardi, Y. Yu, S. Graham, A. Branchizio, S. M. Yoder, M. T. Rock, C. B. Creech, K. M. Edwards, D. Lee, S. Li, I. A. Wilson, A. García-Sastre, R. A. Albrecht, J. E. Crowe Jr., H7N9 influenza virus neutralizing antibodies that possess few somatic mutations. *J. Clin. Invest.* **126**, 1482–1494 (2016).
33. G. Nakamura, N. Chai, S. Park, N. Chiang, Z. Lin, H. Chiu, R. Fong, D. Yan, J. Kim, J. Zhang, W. P. Lee, A. Estevez, M. Coons, M. Xu, P. Lupardus, M. Balazs, L. R. Swem, An in vivo human-plasmablast enrichment technique allows rapid identification of therapeutic influenza A antibodies. *Cell Host Microbe* **14**, 93–103 (2013).
34. A. G. Schmidt, M. D. Therkelsen, S. Stewart, T. B. Kepler, H.-X. Liao, M. A. Moody, B. F. Haynes, S. C. Harrison, Viral receptor-binding site antibodies with diverse germline origins. *Cell* **161**, 1026–1034 (2015).
35. J. Lessler, S. Riley, J. M. Read, S. Wang, H. Zhu, G. J. D. Smith, Y. Guan, C. Q. Jiang, D. A. T. Cummings, Evidence for antigenic seniority in influenza A (H3N2) antibody responses in southern China. *PLOS Pathog.* **8**, e1002802 (2012).
36. M. S. Miller, T. J. Gardner, F. Krammer, L. C. Aguado, D. Tortorella, C. F. Basler, P. Palese, Neutralizing antibodies against previously encountered influenza virus strains increase over time: A longitudinal analysis. *Sci. Transl. Med.* **5**, 198ra107 (2013).
37. K. M. Gostic, M. Ambrose, M. Worobey, J. O. Lloyd-Smith, Potent protection against H5N1 and H7N9 influenza via childhood hemagglutinin imprinting. *Science* **354**, 722–726 (2016).
38. B. Brandenburg, W. Koudstaal, J. Goudsmit, V. Klaren, C. Tang, M. V. Bujny, H. J. W. M. Korse, T. Kwaks, J. J. Otterstrom, J. Juraszek, A. M. van Oijen, R. Vogels, R. H. E. Friesen, Mechanisms of hemagglutinin targeted influenza virus neutralization. *PLOS ONE* **8**, e80034 (2013).
39. J. E. Ledgerwood, C.-J. Wei, Z. Hu, I. J. Gordon, M. E. Enama, C. S. Hendel, P. M. McTamney, M. B. Pearce, H. M. Yassine, J. C. Boyington, R. Bailer, T. M. Tumpey, R. A. Koup, J. R. Mascola, G. J. Nabel, B. S. Graham; VRC 306 Study Team, DNA priming and influenza vaccine immunogenicity: Two phase 1 open label randomised clinical trials. *Lancet Infect. Dis.* **11**, 916–924 (2011).
40. T. Tiller, E. Meffre, S. Yurasov, M. Tsuiji, M. C. Nussenzweig, H. Wardemann, Efficient generation of monoclonal antibodies from single human B cells by single cell RT-PCR and expression vector cloning. *J. Immunol. Methods* **329**, 112–124 (2008).
41. X. Brochet, M.-P. Lefranc, V. Giudicelli, IMGT/V-QUEST: The highly customized and integrated system for IG and TR standardized V-J and V-D-J sequence analysis. *Nucleic Acids Res.* **36**, W503–W508 (2008).
42. E. Hoffmann, G. Neumann, Y. Kawaoka, G. Hobom, R. G. Webster, A DNA transfection system for generation of influenza A virus from eight plasmids. *Proc. Natl. Acad. Sci. U.S.A.* **97**, 6108–6113 (2000).
43. W. H. Organization, Serological Diagnosis of Influenza by Microneutralization Assay, 2010. (World Health Organization, 2013), pp. 1–25.
44. D. N. Mastronarde, Automated electron microscope tomography using robust prediction of specimen movements. *J. Struct. Biol.* **152**, 36–51 (2005).
45. G. Tang, L. Peng, P. R. Baldwin, D. S. Mann, W. Jiang, I. Rees, S. J. Ludtke, EMAN2: An extensible image processing suite for electron microscopy. *J. Struct. Biol.* **157**, 38–46 (2007).
46. S. H. W. Scheres, RELION: Implementation of a Bayesian approach to cryo-EM structure determination. *J. Struct. Biol.* **180**, 519–530 (2012).
47. Z.-Y. Yang, C.-J. Wei, W.-P. Kong, L. Wu, L. Xu, D. F. Smith, G. J. Nabel, Immunization by avian H5 influenza hemagglutinin mutants with altered receptor binding specificity. *Science* **317**, 825–828 (2007).
48. L. Naldini, U. Blömer, F. H. Gage, D. Trono, I. M. Verma, Efficient transfer, integration, and sustained long-term expression of the transgene in adult rat brains injected with a lentiviral vector. *Proc. Natl. Acad. Sci. U.S.A.* **93**, 11382–11388 (1996).
49. Z. Otwinowski, W. Minor, Processing of X-ray diffraction data collected in oscillation mode. *Methods Enzymol.* **276**, 307–326 (1997).
50. P. Emsley, B. Lohkamp, W. G. Scott, K. Cowtan, Features and development of Coot. *Acta Crystallogr. D Biol. Crystallogr.* **66**, 486–501 (2010).
51. P. D. Adams, P. V. Afonine, G. Bunkóczi, V. B. Chen, I. W. Davis, N. Echols, J. J. Headd, L.-W. Hung, G. J. Kapral, R. W. Grosse-Kunstleve, A. J. McCoy, N. W. Moriarty, R. Oeffner, R. J. Read, D. C. Richardson, J. S. Richardson, T. C. Terwilliger, P. H. Zwart, PHENIX: A comprehensive Python-based system for macromolecular structure solution. *Acta Crystallogr. D Biol. Crystallogr.* **66**, 213–221 (2010).
52. E. F. Pettersen, T. D. Goddard, C. C. Huang, G. S. Couch, D. M. Greenblatt, E. C. Meng, T. E. Ferrin, UCSF Chimera—A visualization system for exploratory research and analysis. *J. Comput. Chem.* **25**, 1605–1612 (2004).
53. S. Kumar, G. Stecher, K. Tamura, MEGA7: Molecular evolutionary genetics analysis version 7.0 for bigger datasets. *Mol. Biol. Evol.* **33**, 1870–1874 (2016).

Acknowledgments: We thank J. Weir (FDA) for providing influenza viruses and R. Webby (St. Jude Children's Research Hospital Inc.) for influenza reverse genetics plasmids, H. Anderson (Bioqual Inc.) for animal challenge studies, and D. Ambrozak for help with flow sorting. **Funding:** Support for this work was provided by the Intramural Research Program of the Vaccine Research Center and the Division of Intramural Research, National Institute of Allergy and Infectious Diseases, NIH. This work was supported in part with federal funds from the Frederick National Laboratory for Cancer Research, NIH (under contract HHSN261200800001E). Use of insertion device 22 (SER-CAT) at the Advanced Photon Source was supported by the U.S. Department of Energy, Office of Science, Basic Energy Sciences (under contract W-31-109-Eng-38). **Authors contributions:** S.F.A. designed and performed experiments, analyzed data, performed statistical analysis, coordinated the study, and wrote the manuscript; M.G.J., M.J.C., R.A.G., K.L., E.S.Y., Y.T., A.K.W., M.S.P., and S.R.N. performed experiments and analyzed data; X.C. provided reagents; J.C.B. designed HA probes and generated the HA phylogenetic tree; M.C.C., R.T.B., E.C., G.C., and J.E.L. designed the vaccine trials and provided clinical samples; and M.C.C., M.K., P.D.K., R.A.K., J.R.M., B.S.G., and A.B.M. contributed intellectually to the work and revised the manuscript. **Competing interests:** The NIH has filed a patent application with Patent Cooperation Treaty reference number US2017/030641 related to this study titled "Neutralizing antibodies to Influenza HA and their use and identification." M.G.J., A.K.W., R.T.B., S.F.A., A.B.M., P.D.K., and J.R.M. are inventors on the patent application. **Data and materials availability:** Influenza reverse genetics plasmids were provided by the St. Jude Children's Research Hospital under a material transfer agreement with the NIH. Requests for these reagents should be made to the St. Jude Children's Research Hospital. Antibody sequences are deposited in GenBank. Accession numbers are MF288990 to MF289047. Protein structures are available through the Protein Data Bank (PDB) under PDB codes 5TY6, 5U4R, 5WCA, 5WCC, and 5WCD.

Submitted 20 March 2017
Accepted 26 May 2017
Published 14 July 2017
10.1126/sciimmunol.aan2676

Citation: S. F. Andrews, M. G. Joyce, M. J. Chambers, R. A. Gillespie, M. Kanekiyo, K. Leung, E. S. Yang, Y. Tsybovsky, A. K. Wheatley, M. C. Crank, J. C. Boyington, M. S. Prabhakaran, S. R. Narpala, X. Chen, R. T. Bailer, G. Chen, E. Coates, P. D. Kwong, R. A. Koup, J. R. Mascola, B. S. Graham, J. E. Ledgerwood, A. B. McDermott, Preferential induction of cross-group influenza A hemagglutinin stem–specific memory B cells after H7N9 immunization in humans. *Sci. Immunol.* **2**, eaan2676 (2017).

Science Immunology

Preferential induction of cross-group influenza A hemagglutinin stem–specific memory B cells after H7N9 immunization in humans

Sarah F. Andrews, M. Gordon Joyce, Michael J. Chambers, Rebecca A. Gillespie, Masaru Kanekiyo, Kwanyee Leung, Eun Sung Yang, Yaroslav Tsybovsky, Adam K. Wheatley, Michelle C. Crank, Jeffrey C. Boyington, Madhu S. Prabhakaran, Sandeep R. Narpala, Xuejun Chen, Robert T. Bailer, Grace Chen, Emily Coates, Peter D. Kwong, Richard A. Koup, John R. Mascola, Barney S. Graham, Julie E. Ledgerwood and Adrian B. McDermott

Sci. Immunol. **2**, eaan2676.
DOI: 10.1126/sciimmunol.aan2676

Stemming the tide of influenza

A universal flu vaccine would prevent the need for yearly flu shots, but successful development has been hampered by the diversity and adaptability of the influenza virus. Andrews *et al*. compared B cell responses to the relatively conserved stem region of the influenza cell surface molecule hemagglutinin (HA) in humans vaccinated with either group 2 H7N9 or group 1 H5N1. They found that the stem-targeted memory B cells after H7N9 vaccination recognized both group 1 and group 2 influenza subtypes, whereas H5N1 vaccination induced responses primarily to group 1 subtypes. These data suggest that a group 2 stem immunogen, administered in the proper conditions, would have a higher likelihood of eliciting cross-group protection.